AFFDL-TR-71-4
PART I

AIR CUSHION PRESSURE DURING STIFF-OPERATION FOR AIR CUSHION LANDING SYSTEM

PART I. THEORY

LIT S. HAN

THE OHIO STATE UNIVERSITY RESEARCH FOUNDATION

TECHNICAL REPORT AFFDL-TR-71-4, PART I

MAY 1971

AIR FORCE FLIGHT DYNAMICS LABORATORY
AIR FORCE SYSTEMS COMMAND
WRIGHT-PATTERSON AIR FORCE BASE, OHIO

77

NOTICE

When Government drawings, specifications, or other data are used for any purpose other than in connection with a definitely related Government procurement operation, the United States Government thereby incurs no responsibility nor any obligation whatsoever; and the fact that the government may have formulated, furnished, or in any way supplied the said drawings, specifications, or other data, is not to be regarded by implication or otherwise as in any manner licensing the holder or any other person or corporation, or conveying any rights or permission to manufacture, use, or sell any patented invention that may in any way be related thereto.

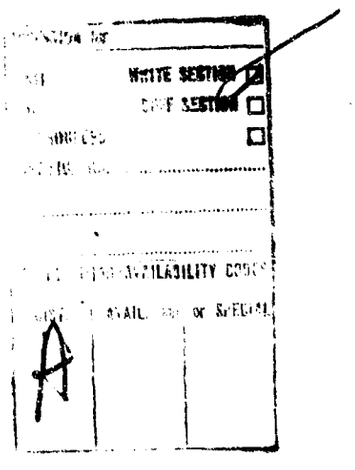

Copies of this report should not be returned unless return is required by security considerations, contractual obligations, or notice on a specific document.

100 - June 1971 - CO305 - 43-71-742

UNCLASSIFIED
Security Classification

DOCUMENT CONTROL DATA - R & D

(Security classification of title, body of abstract and indexing annotation must be entered when the overall report is classified)

1. ORIGINATING ACTIVITY (Corporate Author)	2a. REPORT SECURITY CLASSIFICATION
The Ohio State University Research Foundation Columbus, Ohio	Unclassified
	2b. GROUP

3. REPORT TITLE

Air Cushion Pressure During Stiff-Operation for Air Cushion Landing Systems

4. DESCRIPTIVE NOTES (Type of report and inclusive dates)

July 1969 thru June 1970 (two-part report)

5. AUTHOR(S) (First name, middle initial, last name)

Professor Lit S. Han

6. REPORT DATE	7a. TOTAL NO. OF PAGES	7b. NO. OF REFS
May 1971	73	4

8a. CONTRACT OR GRANT NO.	9a. ORIGINATOR'S REPORT NUMBER(S)
AF33(615)-69-C-1001 b. PROJECT NO. 1369 c. 136907 d.	9b. OTHER REPORT NO(S) (Any other numbers that may be assigned this report) AFFDL-TR-71-4, Part I

10. DISTRIBUTION STATEMENT

This document has been approved for public release and sale; its distribution is unlimited.

11. SUPPLEMENTARY NOTES	12. SPONSORING MILITARY ACTIVITY
	Wright-Patterson Air Force Base, Ohio Air Force FlightDynamics Laboratory

13. ABSTRACT

This report studies the performance characteristics of the air cushioned landing and takeoff system for aircraft during its stiff-operation mode. Stiff-operation is obtained during the early stage of the takeoff period or the later stage of landing. Its chief feature is that the pneumatic supply chamber of bleed air is in almost parallel configuration with the ground. The supply air flows vertically down through the bleed holes and is then deflected outward.

This part of the report contains the theoretical treatment of the problem. The results are in the form of a cushion pressure ratio in terms of the supply (trunk) pressure. Analysis was performed, based on incompressible viscous theory. The second part of the report to be published shortly will detail the experimental results in comparison with theory.

DD FORM 1 NOV 68 1473

Security Classification

14. KEY WORDS	LINK A		LINK B		LINK C	
	ROLE	WT	ROLE	WT	ROLE	WT
Landing gear; ACLS; Launching and alighting systems; Air bearings.						

AIR CUSHION PRESSURE DURING STIFF-OPERATION FOR AIR CUSHION LANDING SYSTEM

PART I. THEORY

LIT S. HAN

FOREWORD

The work reported herein concerns the cushion pressure characteristics for the Air Cushion Landing System under the conditions of stiff-operation, and was performed under United States Air Force Contract No. AF 33(615)-69-C-1001 (Project 1369), with The Ohio State University Research Foundation, Columbus, Ohio.

The content of this part of the report deals with the theoretical calculations. The second part of the report will be concerned with the experimental verification of the theory developed herein. This phase of the work was carried out from July 1969 through June 1970 and the report was released by the author November 1970.

This report has been reviewed and is approved

KENNERLY H. DIGGES
Chief, Mechanical Branch
Vehicle Equipment Division

ABSTRACT

This report studies the performance characteristics of the air-cushioned landing and take-off system for aircraft during its stiff-operation mode. Stiff-operation is obtained during the early stage of the take-off period or the later stage of landing. Its chief feature is that the pneumatic supply chamber of bleed air is in almost parallel configuration with the ground. The supply air flows vertically down through the bleed holes and is then deflected outward.

This part of the report contains the theoretical treatment of the problem. The results are in the form of a cushion pressure ratio in terms of the supply (trunk) pressure. Analysis was performed based on incompressible viscous theory. The second part of the report to be published shortly will detail the experimental results in comparison with theory.

CONTENTS

LIST OF FIGURES AND TABLES

LIST OF FIGURES AND TABLES (cont.)

SYMBOLS

A_r	area of orifices/total area of seal
C	pressure gradient parameter, see equation 9a
$C_oC_1\ldots$	coefficients of C, see equation 22
C_d	coefficient of discharge for orifice
H	clearance above ground
L	seal length, see Figure 1
p	pressure
p_a, p_c, p_t	ambient, cushion-space and trunk pressures psia
R_e	Reynolds number (v_w H/ν)
u	velocity along x-axis (parallel to the ground)
u_a	average velocity of u, ($v_w x/H$)
v	velocity along y-axis (perpendicular to the ground)
v_w	injection or suction velocity
x,y	coordinates in Figure 2
$\bar{y}$	non-dimensional y-coordinate (y/H)
ν	kinematic viscosity
μ	dynamic viscosity
ρ	density
ε	$(1/\sqrt{R_e})$
δ	boundary layer thickness
$\bar{\delta}$	non-dimensional boundary layer thickness (δ/H)
γ, β, η	temporary coefficients, see equation (15), (16)

I INTRODUCTION

The air-cushioned landing system for aircraft is based on a simple fluid dynamic phenomenon - the momentum principle. It has the all important advantage of being able to operate over terrains other than paved runways or over water. Furthermore, it obviates the complicated retractable gear system.

The construction consists of a retractable pneumatic bag shaped in a toroidal manner and fastened to the fuselage. The pneumatic bag made from rubber-like elastic material is provided with air bleed-holes and can be inflated by a low-pressure high-volume air source. During operational periods, i.e., takeoff or landing, the inflated bag forms a seal between the supporting base area of the aircraft and the ground. In this manner, a cushion space is formed. The pressurized air is forced through the distribution holes and is deflected, because of the symmetry in geometry to form a peripheral ground jet. The outward momentum of the ground jet creates a positive air pressure in the cushion space or the base region. It is this positive pressure that supports the aircraft weight during takeoff or landing operation. Figure 1 depicts the schematics of such a system together with the current nomenclature.

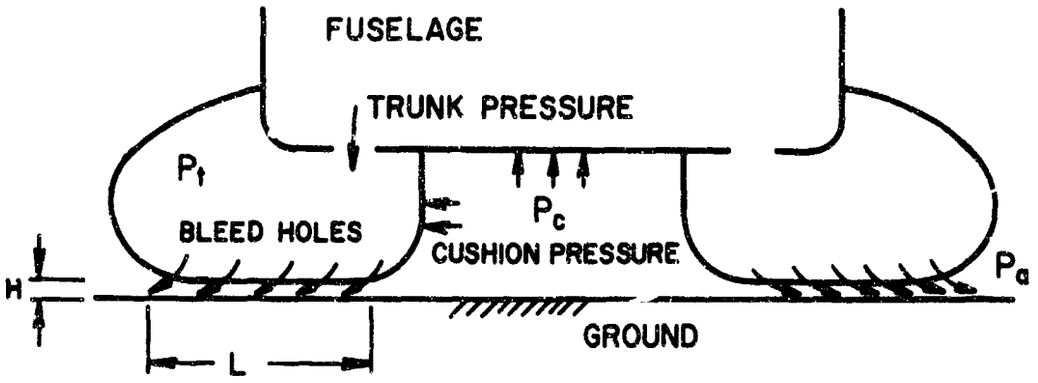

FIGURE 1 SCHEMATICS OF AIR-CUSHIONED LANDING SYSTEM

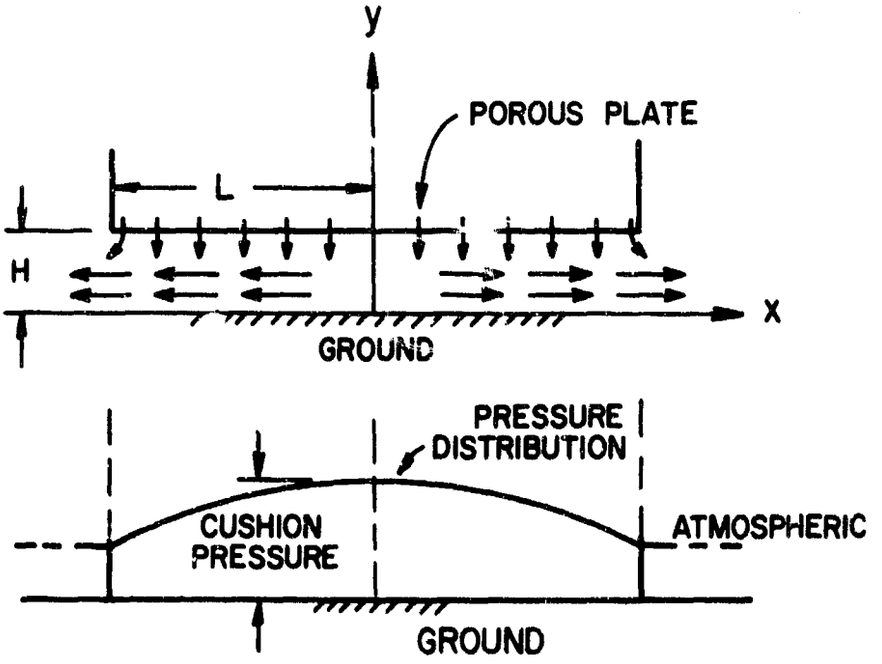

FIGURE 2. SIMPLIFIED FLUID DYNAMIC MODEL FOR STIFF OPERATION

While the practicality of such a landing system has been amply demonstrated in successful flight tests by the Bell Aerosystems program, further research, testing and gathering of engineering data are required in order to obtain more precise information for the optimum design of such a system for various modes of operations. Some of the obvious modes of operations may be mentioned: viz. during landing operation the attitude of the aircraft may necessitate a landing with a fixed pitch angle or a fixed roll angle. The cushion seal is no longer of a uniform height around the periphery. This mode of operation may considerably alter the fluid dynamic behavior near the base region and hence the maneuverability of the aircraft. Alternatively the ground jet distribution may be influenced by a crosswind which again may change the handling characteristics of the aircraft in question. Aside from these factors it is to be noted that the locations, spacings and sizes of the bleed-holes have not yet been optimized although some preliminary work was reported by Earl in the report by Bell [1]*. Furthermore, it was observed that the pneumatic bag experienced some breathing-mode vibrations during its inflation stage which is indicative of the complexities of the mechanics of deformation of such a

---

*Numbers in brackets are reference numbers.

toroidal elastic enclosure. The exact shape of the cushion bag under pressure may be of importance in that the cushion pressure distribution in the base area may be greatly influenced by the deformed shape. Similarly, a number of design considerations dealing with the controlled bleed-flow distribution in various portions of the pneumatic bag may be mentioned. The controlled distribution may be accomplished by compartmentalizing the pneumatic bag; each compartment having its own pressure. This scheme can be accomplished by a proper valving and ducting and can be used to control and direct the aircraft attitude. The preceding-mentioned phenomena are noted herein to indicate the need for further studies and refinements and will be more fully elaborated upon in a later report.

The present study described in this report is, however, concerned with a particular mode of operation known as the stiff-operation which takes place when the pneumatic bag is very close to the ground. The air seal formed becomes a long (in the air flow direction) passage with very small height (clearance to the ground). Figure 1 shows the schematics of the various major components comprising the air-cushion system. For the stiff-operation mode, the bleed air is directed along the small passage outward leaving the cushion space relatively undisturbed. Consequently, the fluid dynamic behavior can be very well simulated by

assuming the cushion space to be a stationary area and the two air passages can be brought together as shown in Figure 2 in which the ground is replaced by a solid plane on the x-axis and the source of air injection is replaced by a porous plate at a fixed distance H above the ground. The plate has a length of 2L. The injected air is divided along the y-axis. The pressure at either end of the porous plate is taken to be atmospheric. The objective of the present study is to analyze the pressure along the passage. Since at x = 0 along the y-axis the flow is zero due to symmetry, hence the pressure there shall be taken as the pressure in the cushion space which is assumed to have no motion. The injection of air is to take place with a uniform rate independent of x. The latter assumption will be removed later in this report. A subsequent report will discuss and analyze the fluid dynamics when the former assumption is removed, i.e. there is induced motion of the air in the cushion space.

II. ANALYSIS

Employing the assumption of an incompressible fluid model and two-dimensional flow the equations of motion and of continuity are:

$$uu_x + vu_y = -p_x/\rho + \nu\nabla^2 u \tag{1}$$

$$uv_x + vv_y = -p_y/\rho + \nu\nabla^2 v \tag{2}$$

$$u_x + v_y = 0 \tag{3}$$

The boundary conditions associated with the preceding equations are:

$$u = v = 0 \qquad y = 0 \tag{4a}$$

$$u = 0 \qquad y = H \tag{4b}$$

$$v = -v_w \qquad y = H \tag{4c}$$

III. UNIFORM INJECTION CASE

Since the flow in the passage is caused by the injection at the upper boundary the flow velocity in the x-direction must be linearly proportional to x, the distance from the line of symmetry, for a constant rate of injection, i.e. $v = -v_w$ at $y = H$. Consequently, the stream function Ψ can be written as:

$$\Psi = v_w \times F(\bar{y}) \tag{5}$$

where $\bar{y} = y/H$

$$v = -v_w F \tag{6}$$

$$u = (v_w x/H) F' \tag{7}$$

Substitution of the above relations into equations (1) and (2) yields:

$$F'^2 - FF'' = -(H^2 p_x/\rho v_w^2 x) = F'''/Re \tag{8}$$

$$FF' = -(H\, p_y/\rho v_w^2) - F''/Re \tag{9}$$

where $Re = (H\, v_w/\nu)$

Equation (9) states that p_y is independent of x; hence p_x is independent of y. In equation (8) the first term on the right-hand side is, therefore, independent of y and can be regarded as a constant, or

$$-(H^2 p_x/\rho v_w^2 x) = C \tag{9a}$$

the principal equation concerned in this report is then

$$F'^2 - FF'' = C + F'''/Re \tag{10}$$

the boundary conditions are

$$F(0) = F'(0) = F'(1) = 1 - F(1) = 0 \tag{11}$$

In equation (10) the Reynolds number is a parameter to be arbitrarily specified and there are four boundary conditions in (11) for the third-order equation. The constant C analogous to an eigen-value in a linear differential equation is to be determined as well. Its value is, of course, dependent on the Reynolds number.

Low Reynolds Number Case

For very low Reynolds numbers the inertia terms on the left-hand side of equation (1) can be ignored since they are of the second-order nature and the equation reduces to

$$F''' = -C\ Re \tag{12}$$

with a solution

$$F = -(2\bar{y}^3 - 3\bar{y}^2)\ (C\ Re/12) \tag{13}$$

which satisfied the first three boundary conditions of (11) and the last condition is fulfilled by

$$C = 12/Re \tag{14}$$

The velocity profile from $\bar{y} = 0$ to $\bar{y} = 1$ is given by

$$F' = \bar{y}\ (1-\bar{y})\ (C\ Re/2) \tag{14a}$$

which is symmetrical about the mid-channel position $\bar{y} = 1/2$

thus exhibiting no convective effect from the injection side $\bar{y} = 1$.

The velocity profiles for very low Reynolds number are graphically shown in Figures 3, 4, ... for increasing values of the Reynolds number. The profiles exhibit symmetry about the midpoint of the flow channel, characterizing the absence of the inertia effect. The pressure distribution along the channel is solely caused by the frictional effect and can be calculated directly from equations (9a) and (14). Equating these two equations,

$$-H^2 p_x/(\rho\ v_w^2\ x) = C = 12/(v_w H/\nu)$$

Denoting the atmospheric pressure by p_a, the pressure distribution is obtained as

$$(p-p_a) = (6\mu\ v_w/H^3)\ (L^2 - x^2)$$

The maximum pressure occurs at the mid-channel $x = 0$ where the velocity is zero. In an approximate sense it is also the pressure in the cushion space. Denoting it by p_c, the value is

$$p_c - p_a = 6\mu\ v_w\ L^2/H^3$$

This equation may be used either to calculate the cushion pressure or the injection velocity v_w.

Arbitrary Reynolds Number Case

Studies similar to the present problem have been undertaken by a number of investigators although for different

applications from that contemplated in the present case. Yuan and Finkelstein [2] studied the problem of flow in a circular tube with porous wall. The resulting equation governing the velocity distribution is quite similar to (10) and (11). Their method consists of solving for the stream function in an ascending series of Re for small Reynolds number or series of (1/Re) for large Reynolds numbers. Because of the series method of solution a large number of terms are required for accurate evaluation of the velocity profiles. Consequently, Morduchow [3] devised an integral method modeled after the K. ın-Pohlhausen method to solve the problem posed in [2]. The method is well known to be reliable only when it can be shown to agree with some known exact solutions. A more rigorous treatment of the similar problem has recently been given by White et al [4]. The last-mentioned work solved the problem by an infinite series in terms of the physical coordinates. The method is conceptually exact but is tedious to execute.

In the present study the method of solution of equations (10) and (11) are made exact both conceptually and numerically. The execution of the solution turns out to be quite simple. In the first place equations (10) and (11) constitute a two fixed-point boundary value problem with an associated eigen-value. The "eigen-value" C in

equation (10) together with the arbitrary parameter Re appears to be complicated; but in reality they simplify the problem as can be seen as follows:

Let $$F(\bar{y}) = \beta f(\gamma\bar{y}) \tag{15a}$$

$$\eta = \gamma\bar{y}$$

Equation (10) becomes

$$\beta^2 \gamma^2(f'^2 - ff'') = C + \beta\gamma^3 f'''/Re$$

Putting $\beta^2 \gamma^2 = C = \beta\gamma^3/Re$ the following results:

$$\beta = C^{1/4}/Re^{1/2} \tag{16a}$$

$$\gamma = C^{1/4} Re^{1/2} \tag{16b}$$

and the equation for f now reads

$$f'^2 - ff'' = 1 + f''' \tag{17}$$

which turns out to be the well-known Falkner-Skan equation. However, the boundary conditions are:

$$f(0) = f'(0) = 0$$

$$f(C^{1/4} Re^{1/2}) = Re^{1/2} C^{1/4}$$

$$f'(C^{1/4} Re^{1/2}) = 0 \tag{18}$$

Now the behavior of the function f subject to the first two boundary conditions of (18) is well known. For $f''(0) > 1.2326$, f' increase from zero monotonically. For $f''(0) < 1.2326$, the graph of $f' \sim \eta$ exhibits a maximum with $f' < 1$ and the f'-curve crosses the η-value. Taking advantage of these known properties, equation (17) with (18) as its boundary conditions may be solved by <u>assuming</u> an arbitrary value of $f''(0)$ between 0 and 1.2326.

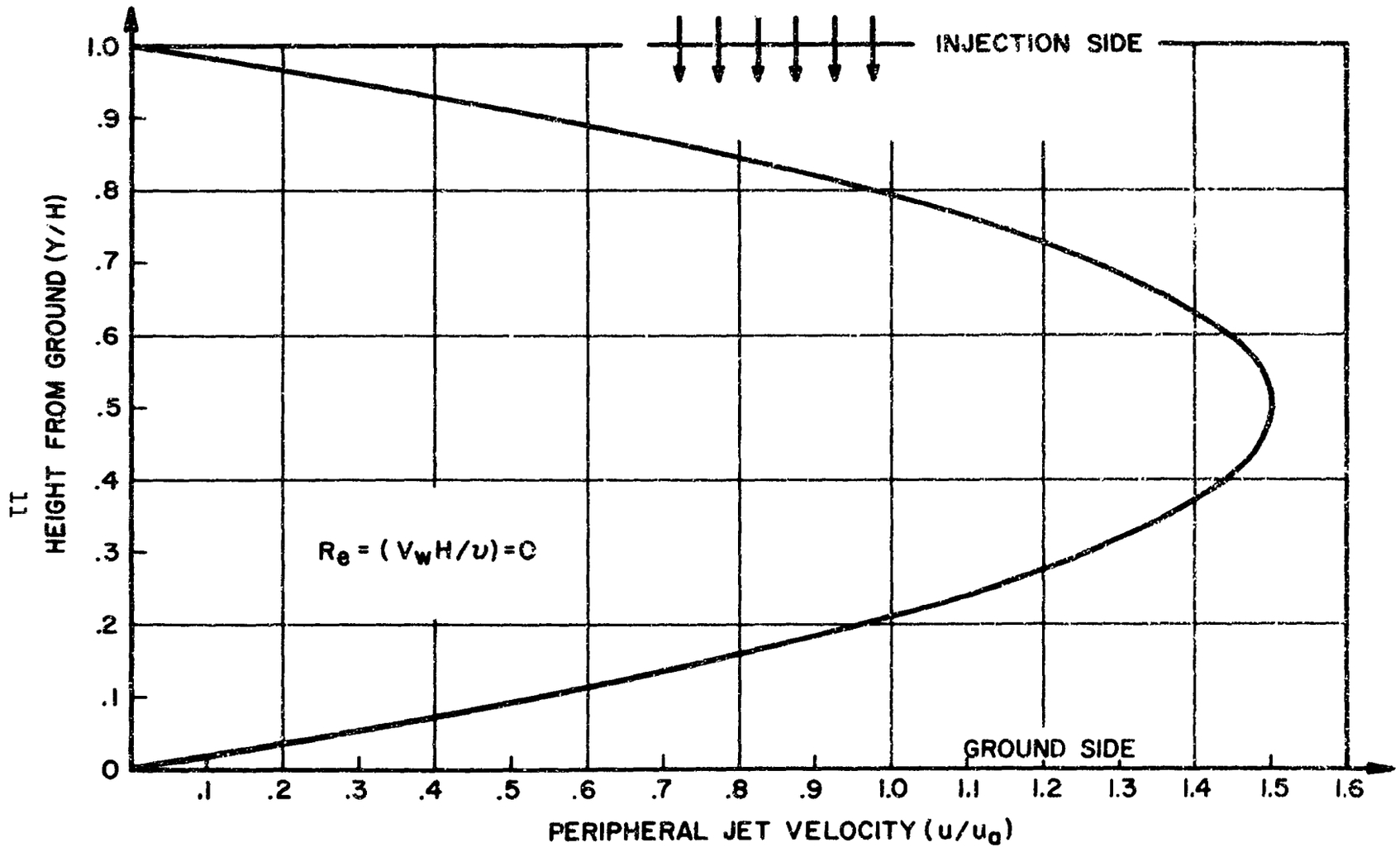

FIGURE 3 VELOCITY DISTRIBUTION ACROSS CHANNEL-SEAL ($R_e = 0$)

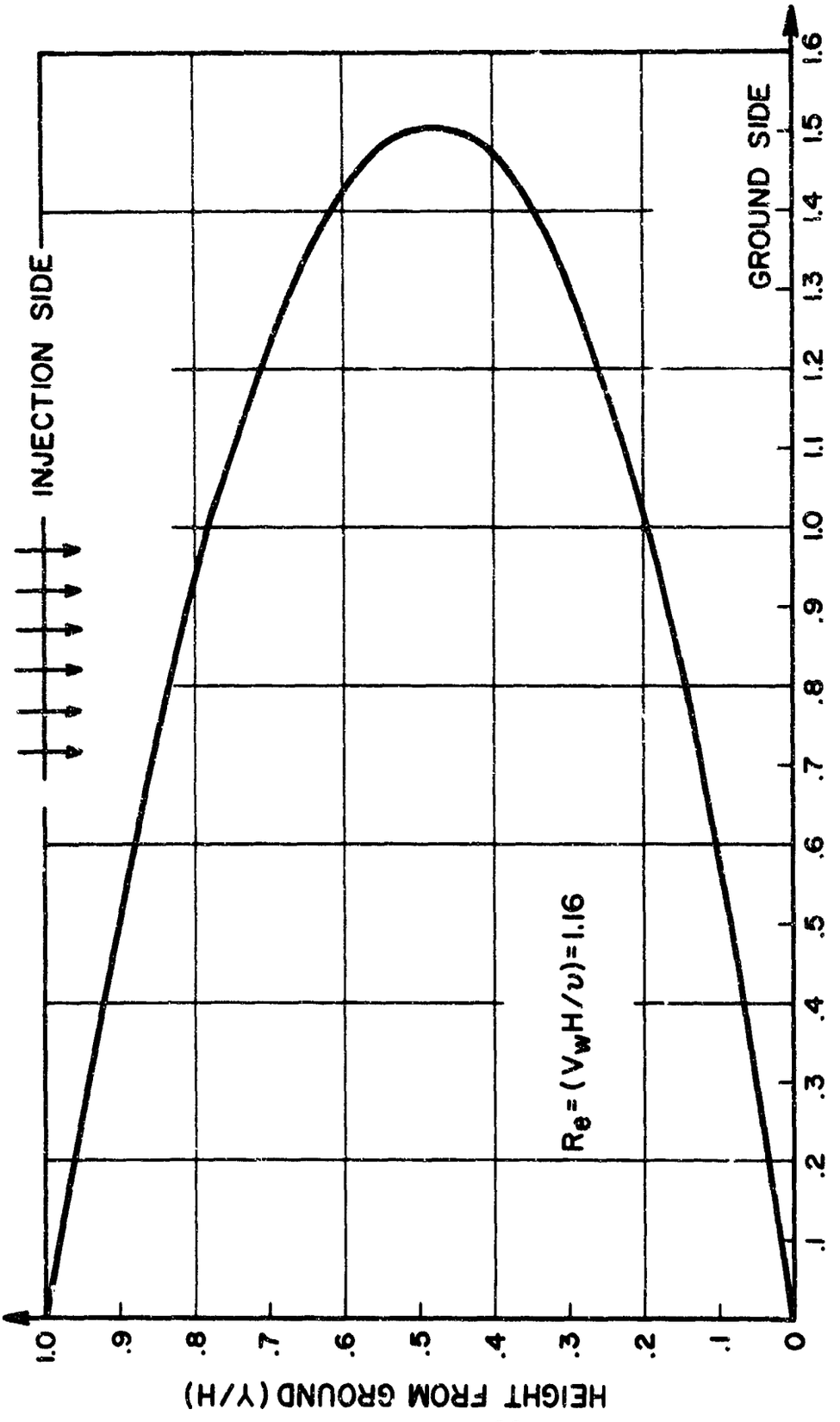

FIGURE 4 VELOCITY DISTRIBUTION ACROSS CHANNEL-SEAL ($R_e = 1.16$)

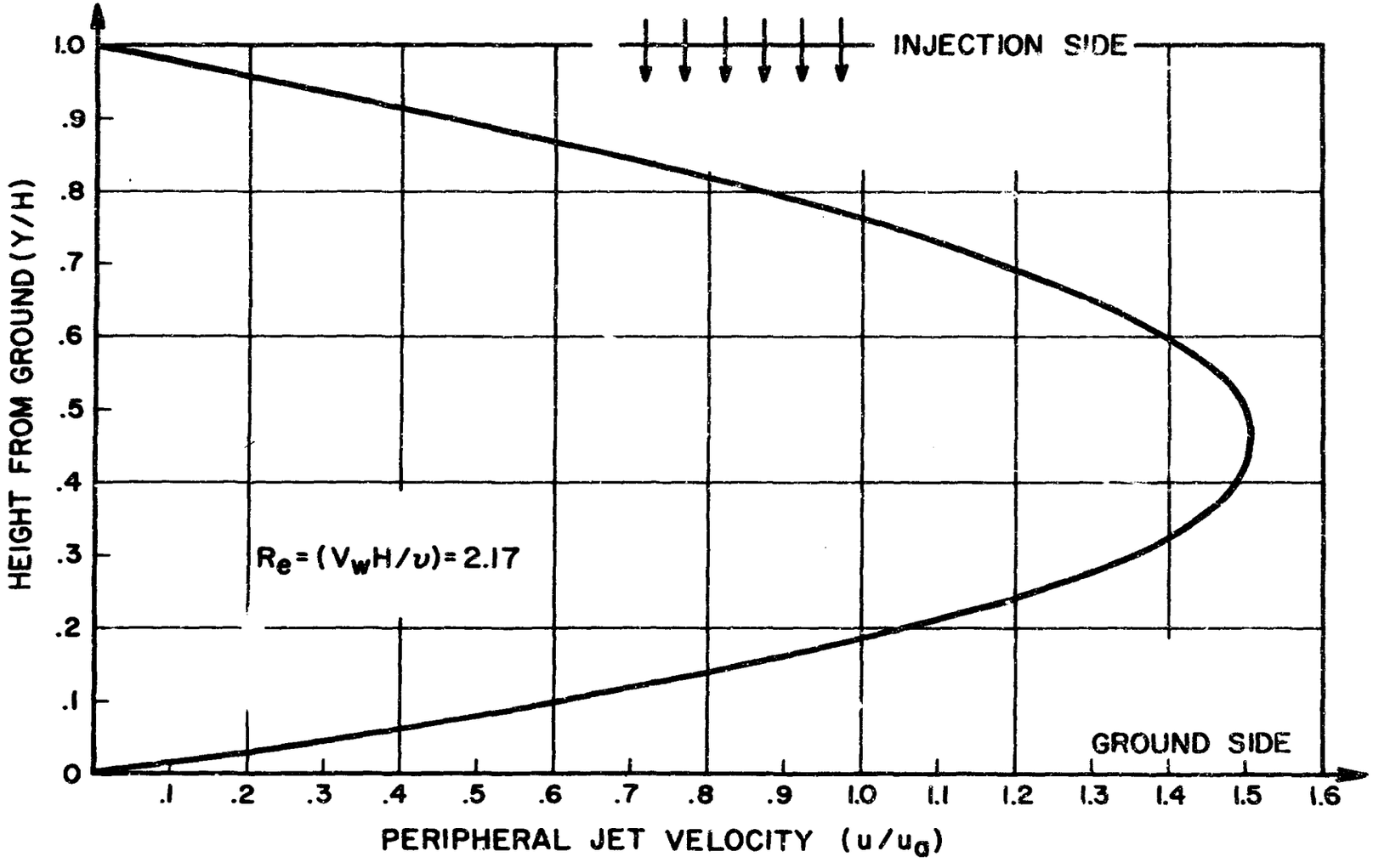

FIGURE 5 VELOCITY DISTRIBUTION ACROSS CHANNEL-SEAL (R_e = 2.17)

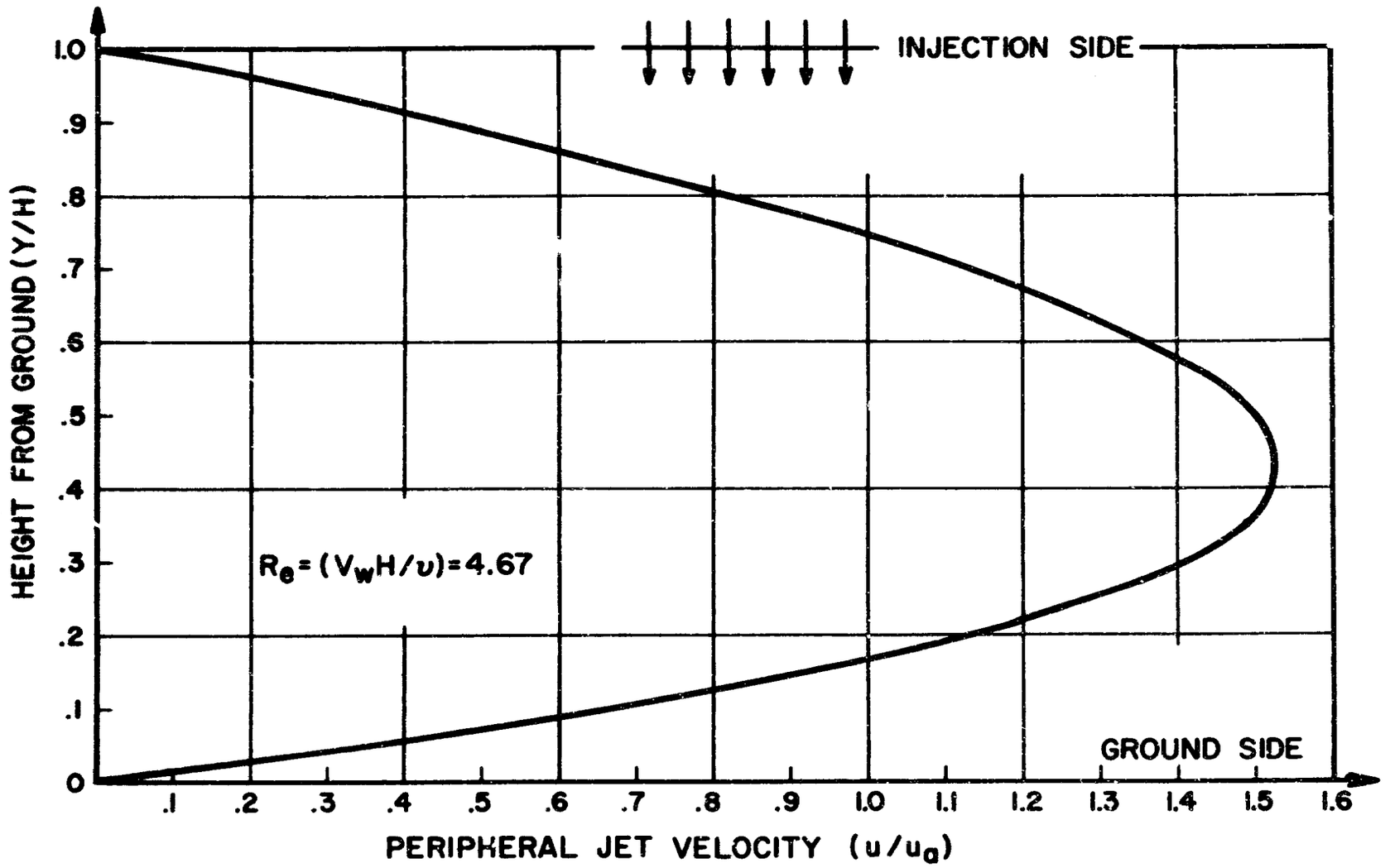

FIGURE 6 VELOCITY DISTRIBUTION ACROSS CHANNEL-SEAL ($R_e = 4.67$)

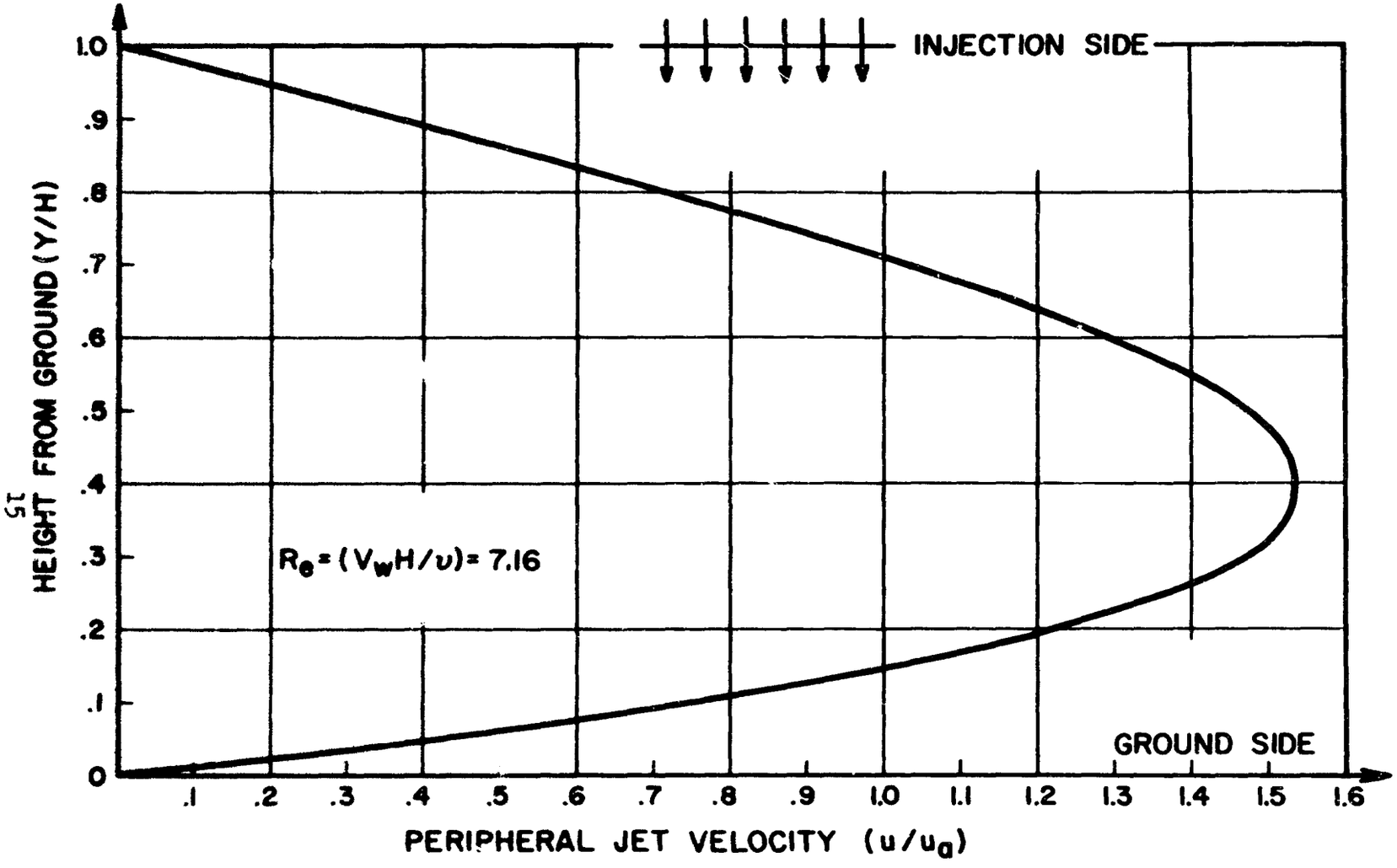

FIGURE 7 VELOCITY DISTRIBUTION ACROSS CHANNEL-SEAL ($R_e = 7.16$)

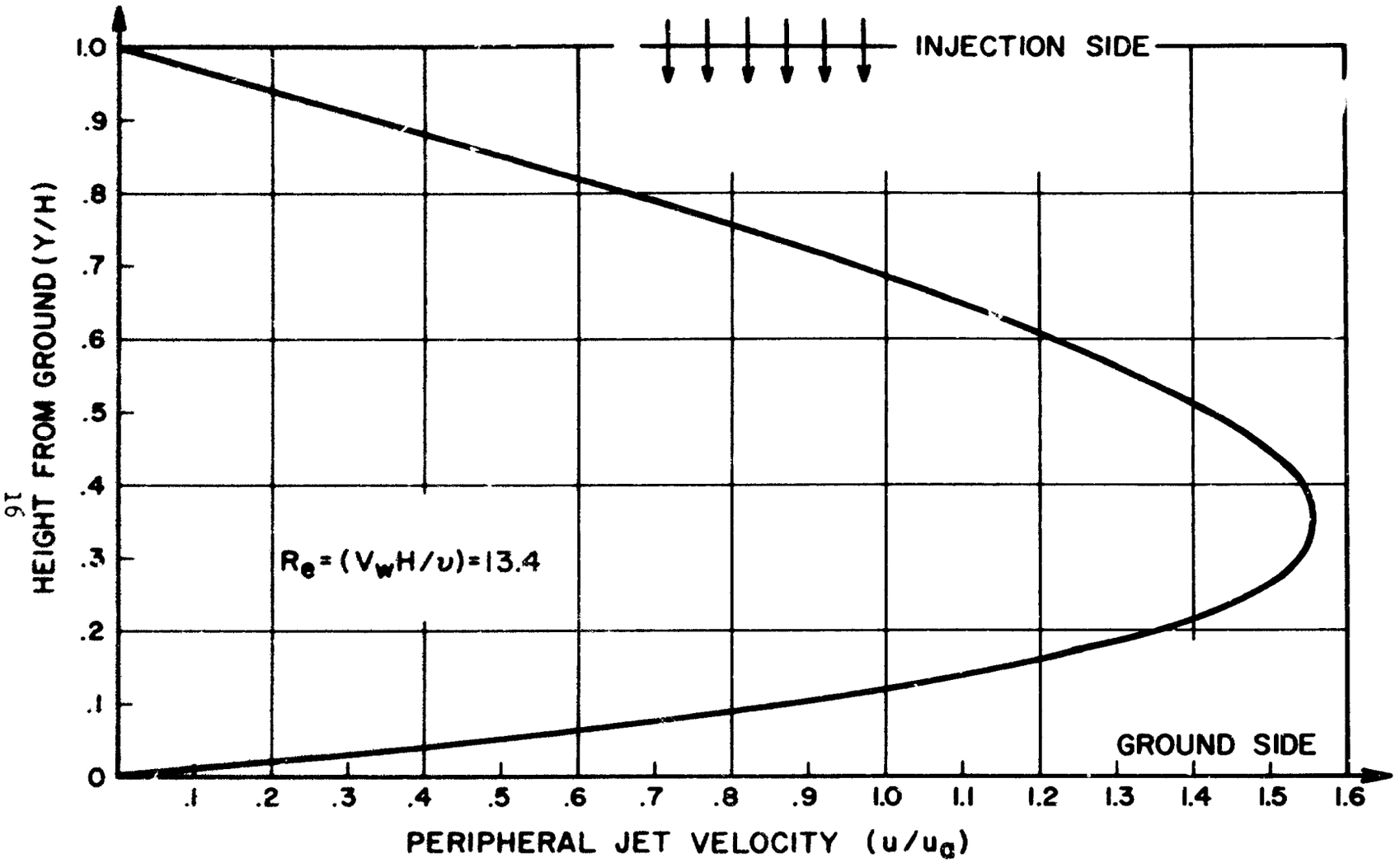

FIGURE 8 VELOCITY DISTRIBUTION ACROSS CHANNEL-SEAL ($R_e = 13.4$)

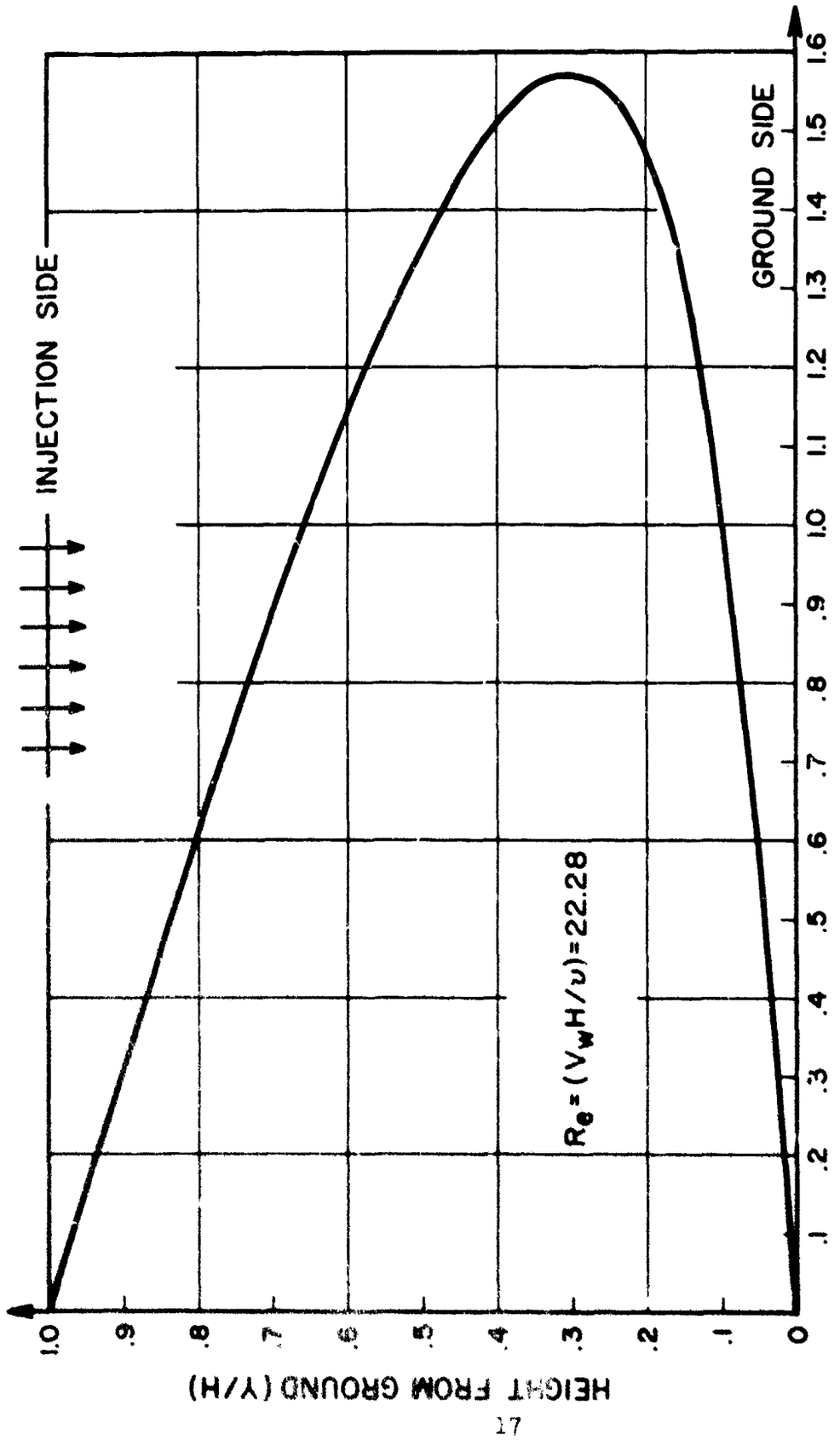

FIGURE 9 VELOCITY DISTRIBUTION ACROSS CHANNEL-SEAL (R_e = 22.28)

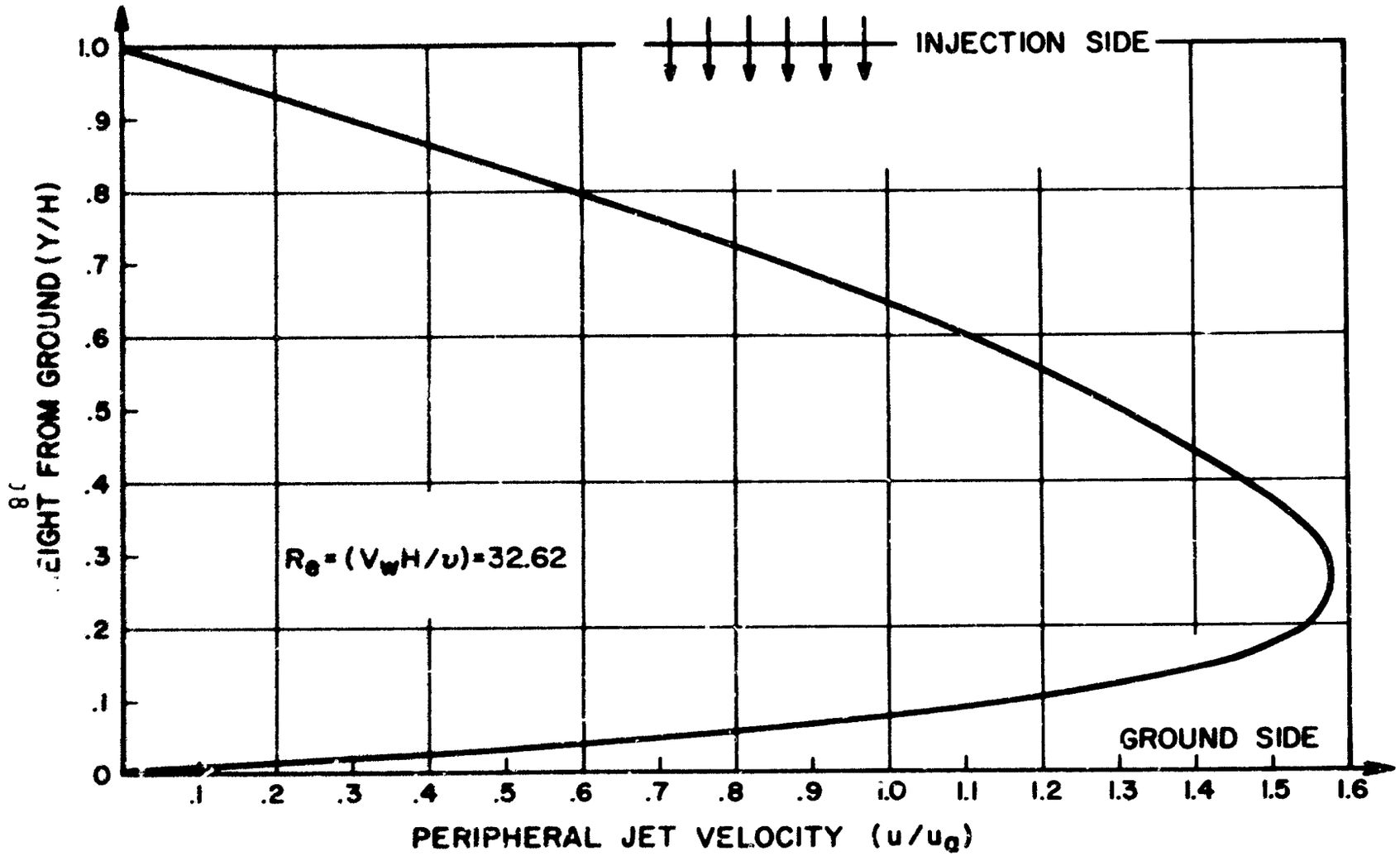

FIGURE 10 VELOCITY DISTRIBUTION ACROSS CHANNEL-SEAL (R_e = 32.62)

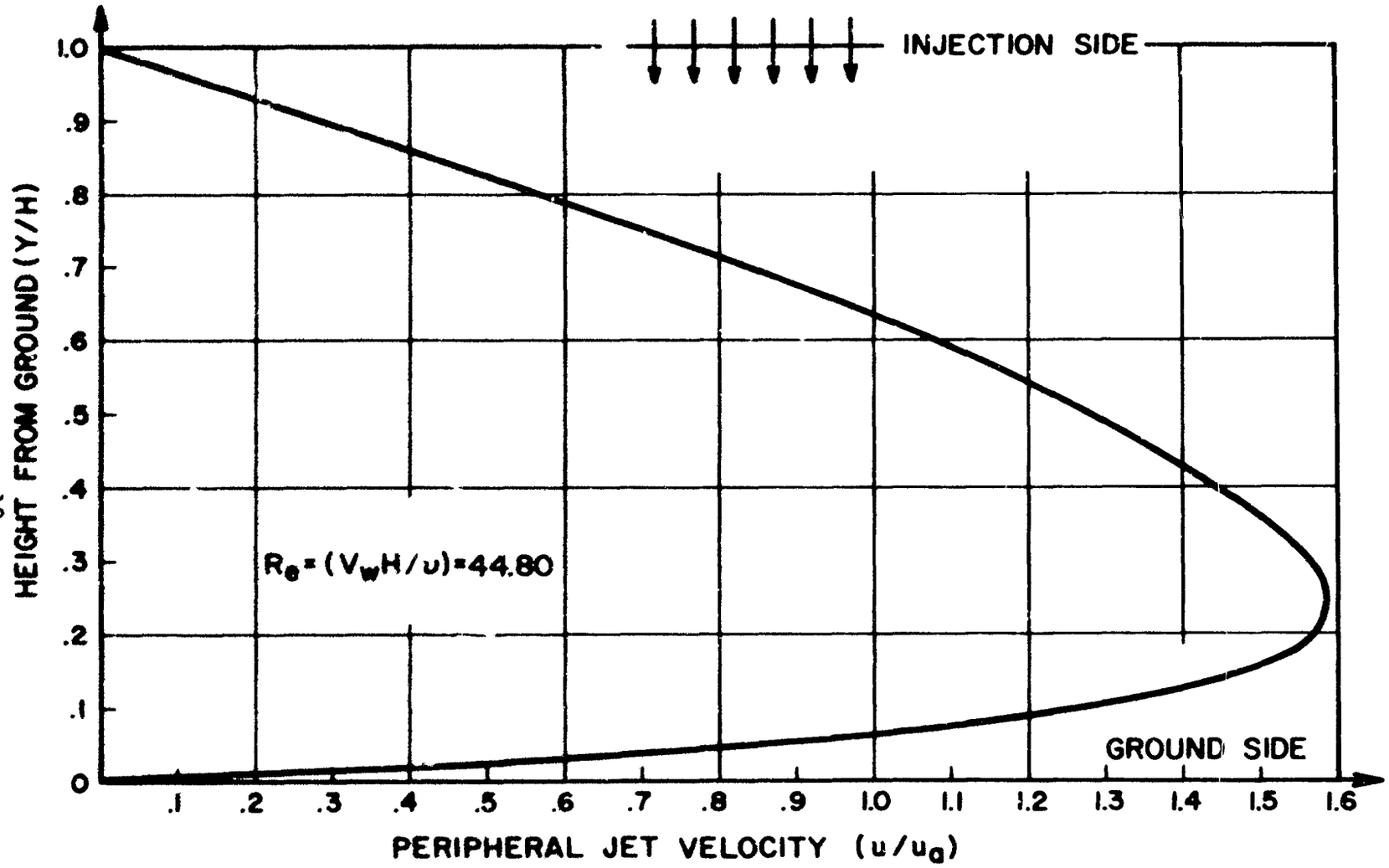

FIGURE 11 VELOCITY DISTRIBUTION ACROSS CHANNEL-SEAL (R_e = 44.80)

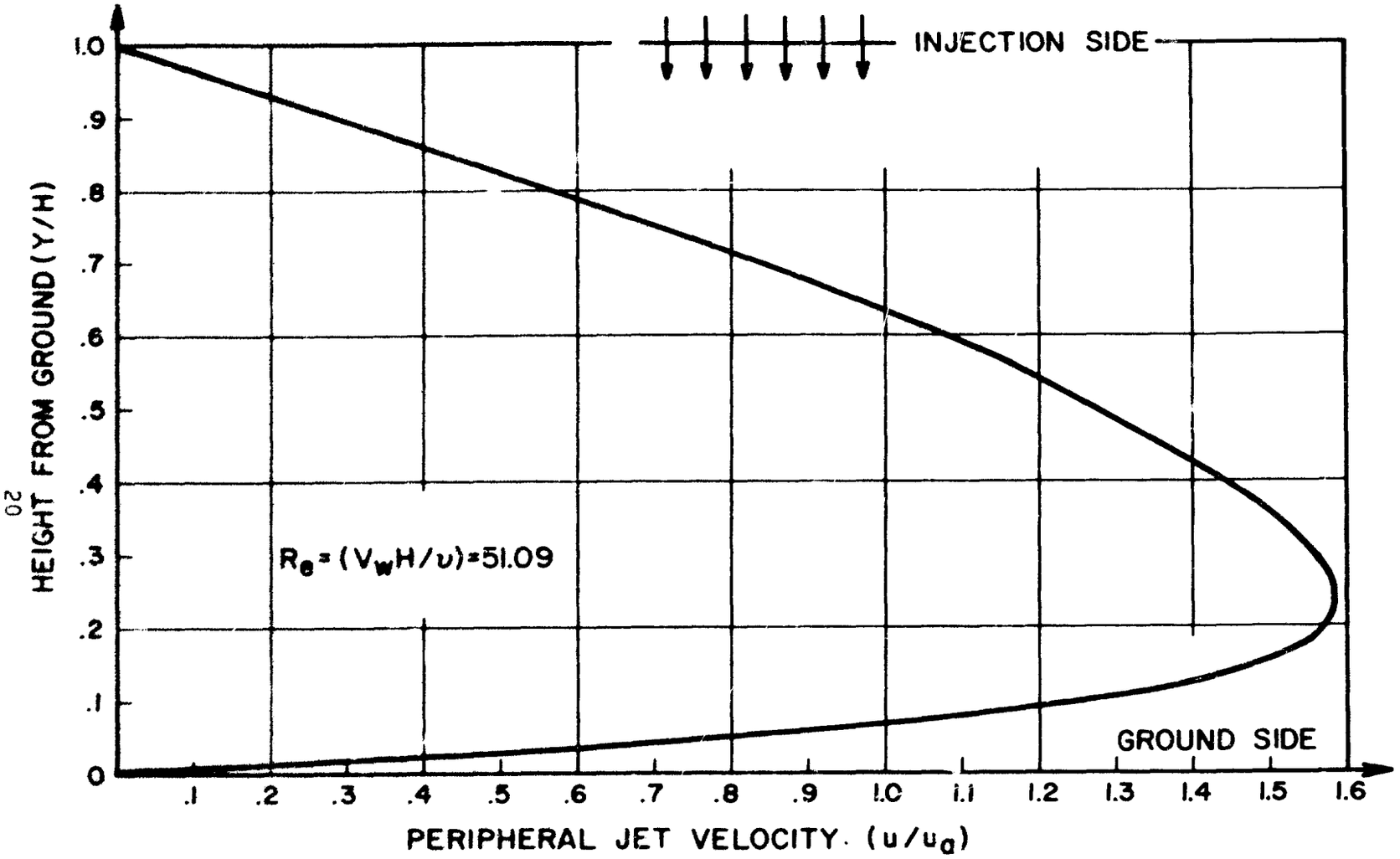

FIGURE 12 VELOCITY DISTRIBUTION ACROSS CHANNEL-SEAL (R_e = 51.09)

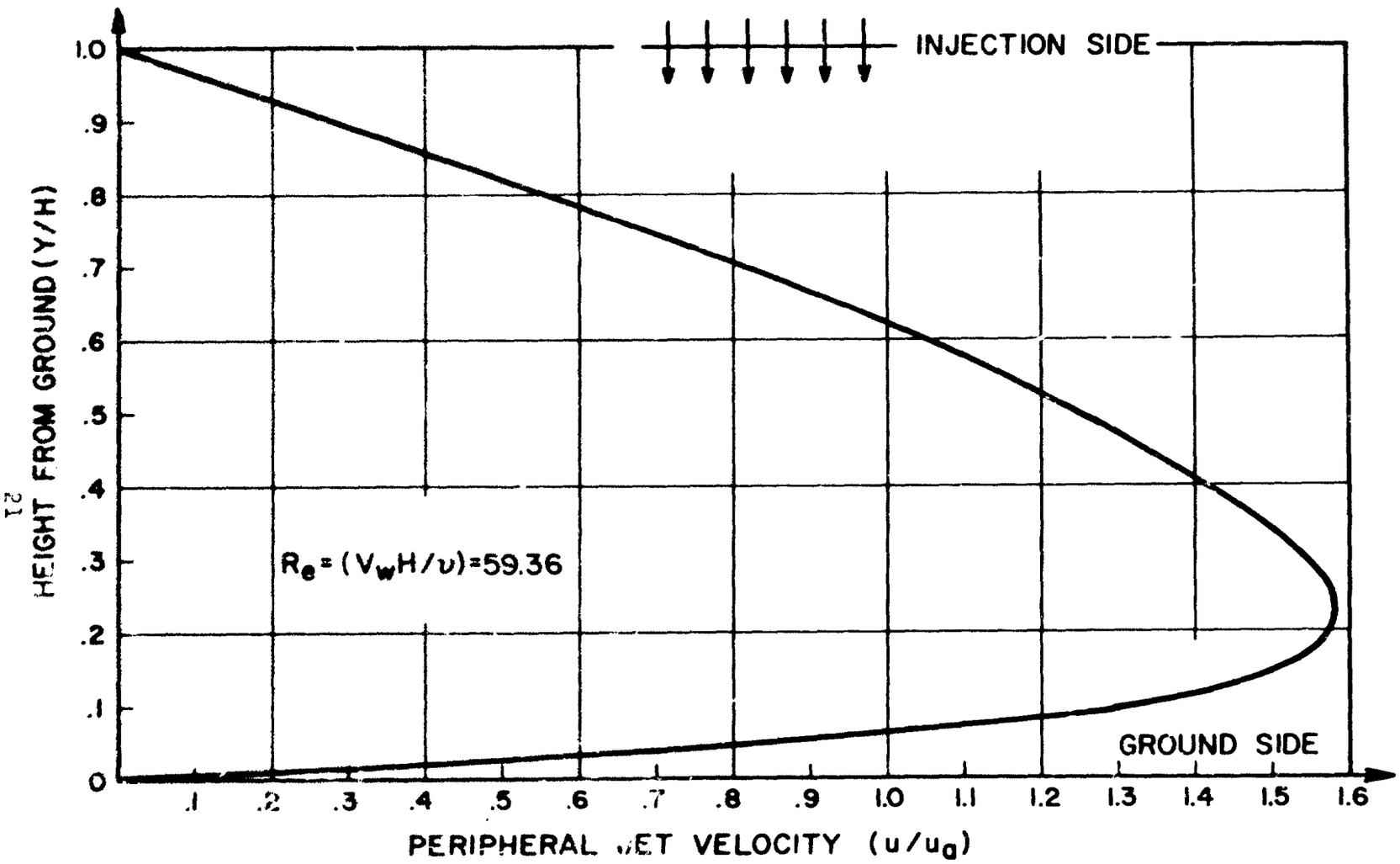

FIGURE 13 VELOCITY DISTRIBUTION ACROSS CHANNEL-SEAL ($R_e = 59.36$)

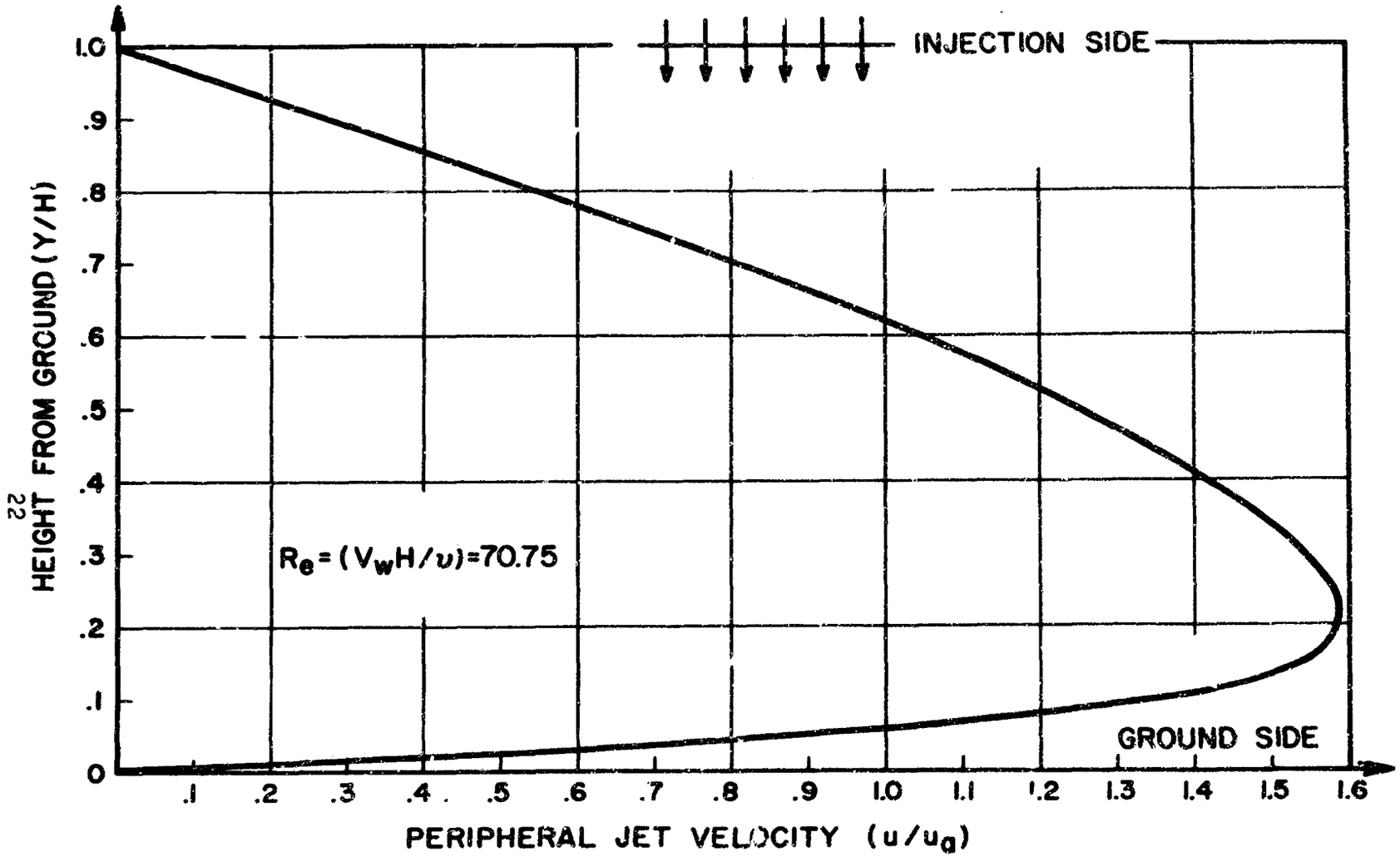

FIGURE 14 VELOCITY DISTRIBUTION ACROSS CHANNEL-SEAL (R_e = 70.75)

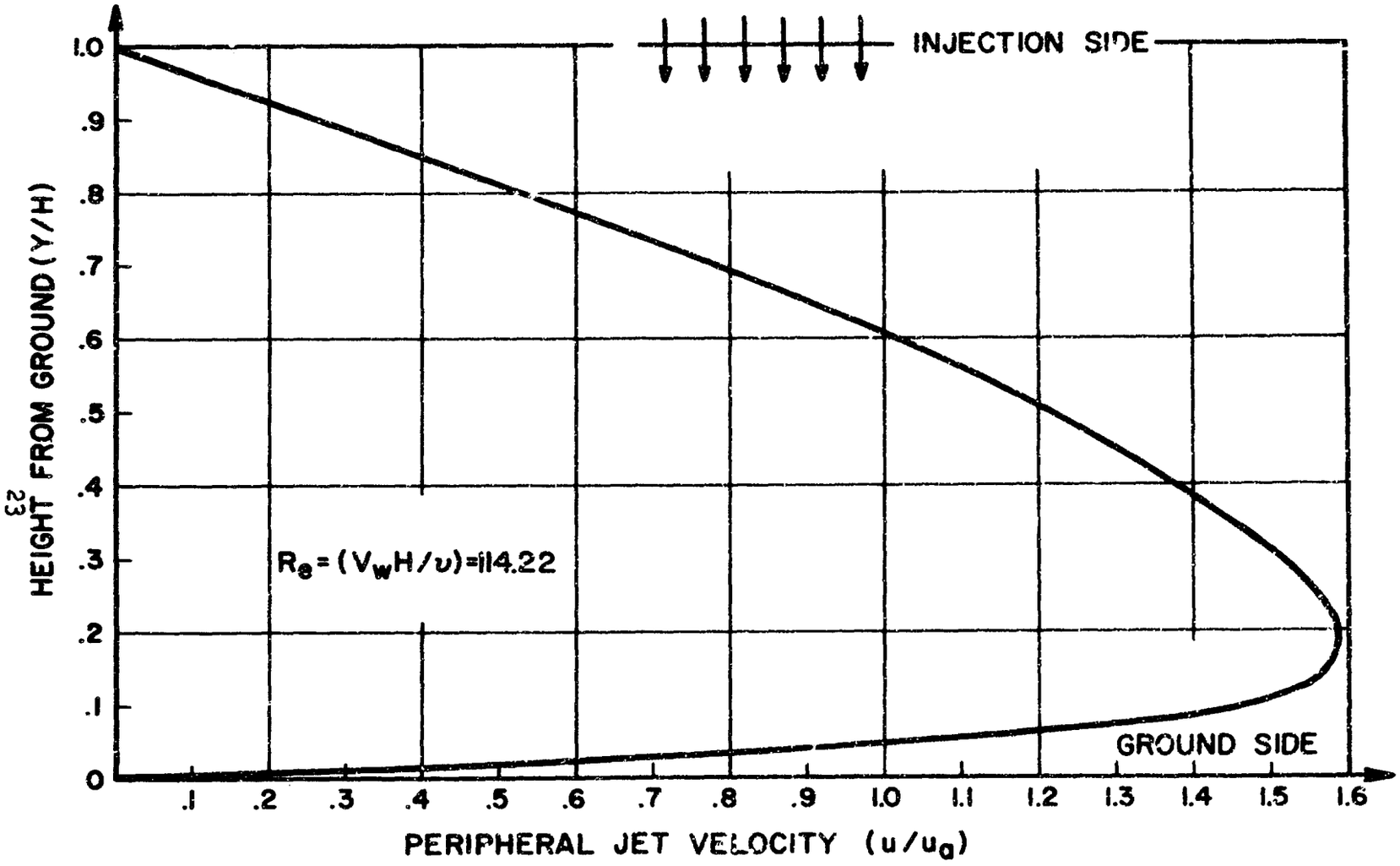

FIGURE 15 VELOCITY DISTRIBUTION ACROSS CHANNEL-SEAL ($R_e = 114.22$)

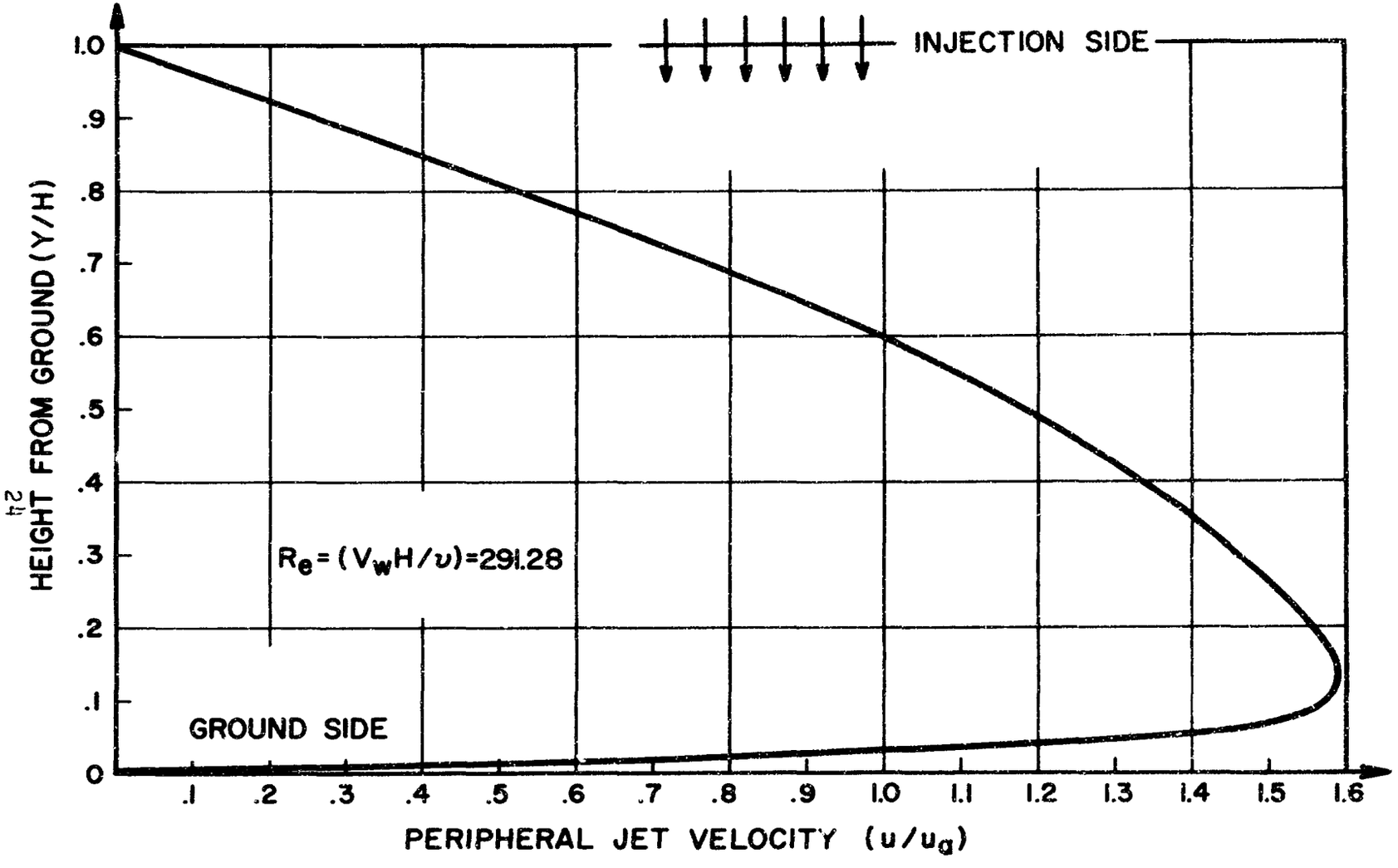

FIGURE 16 VELOCITY DISTRIBUTION ACROSS CHANNEL-SEAL (R_e = 291.28)

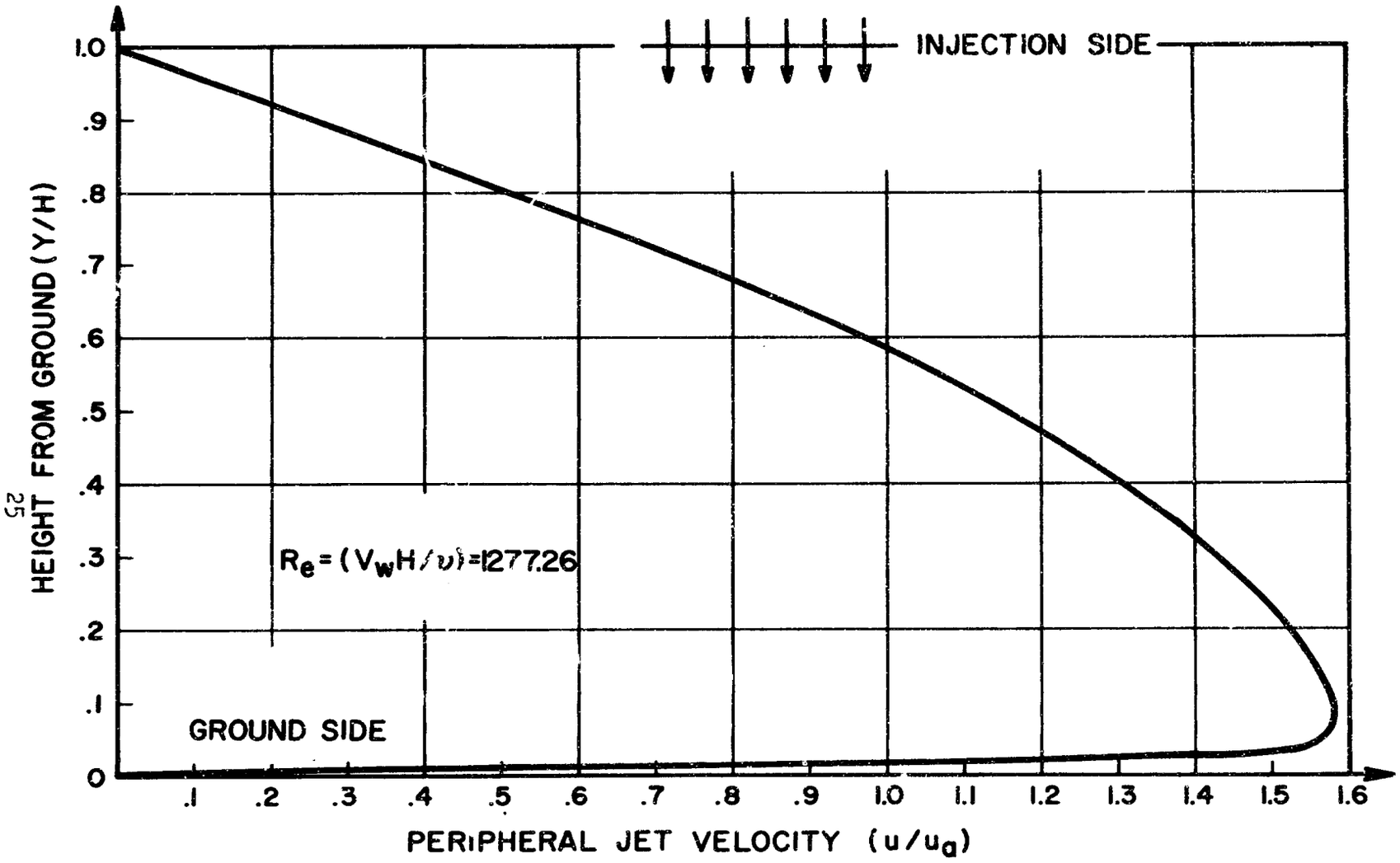

FIGURE 17 VELOCITY DISTRIBUTION ACROSS CHANNEL-SEAL (R_e = 1277.26)

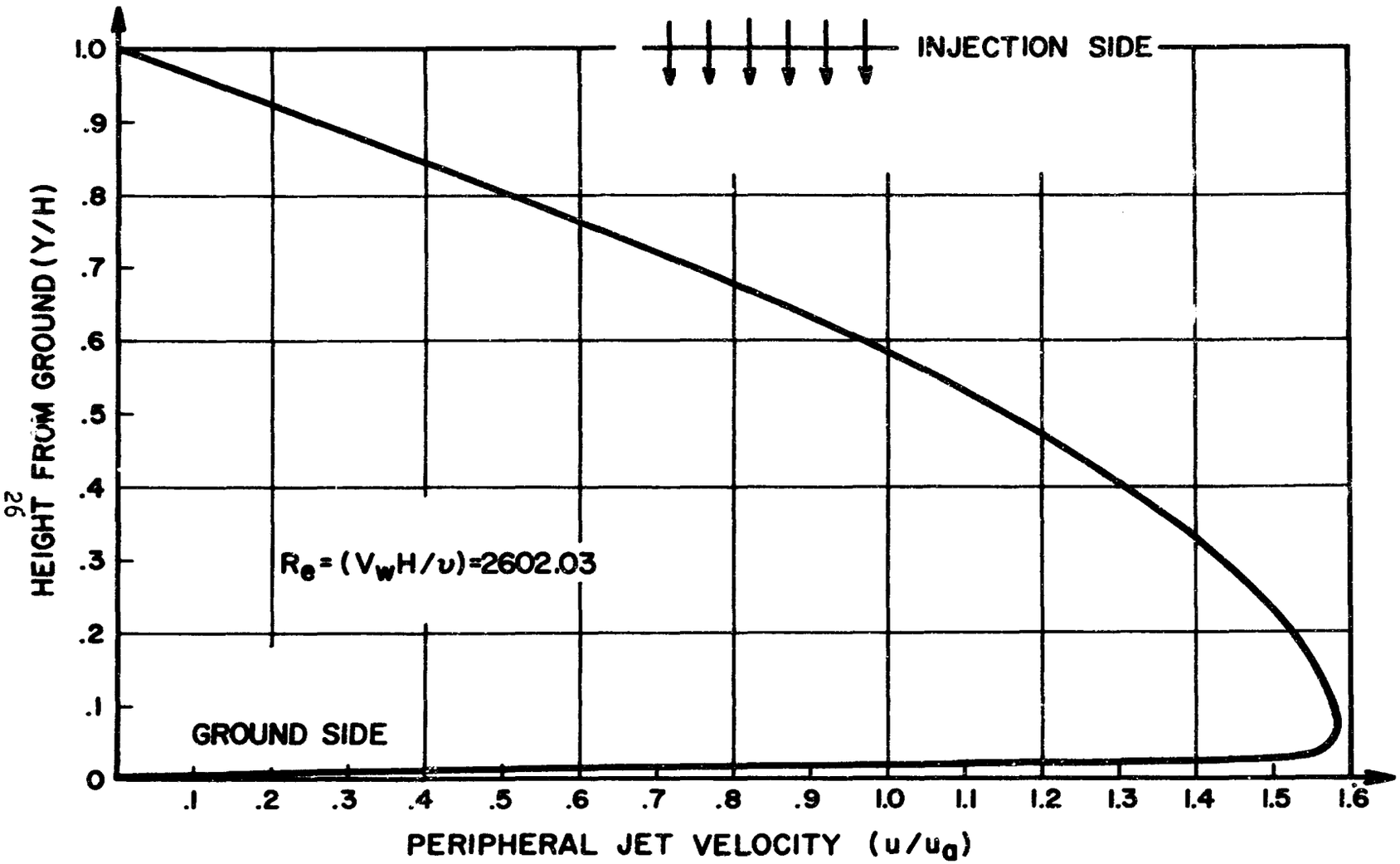

FIGURE 18 VELOCITY DISTRIBUTION ACROSS CHANNEL-SEAL (R_e = 2602.03)

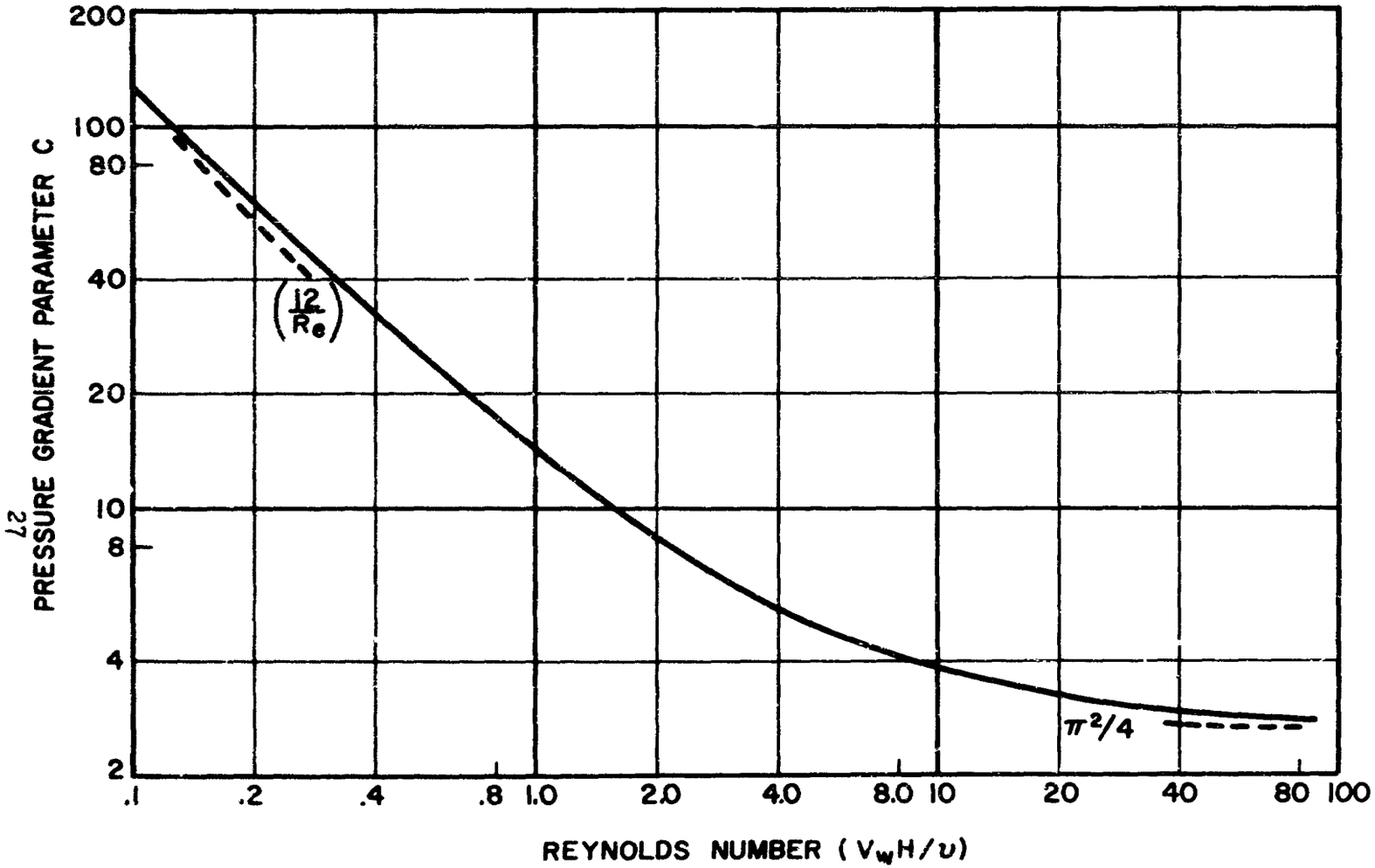

FIGURE 19 PRESSURE GRADIENT PARAMETER vs. REYNOLDS NUMBER IN SEAL-CHANNEL. $C = -(H^2 P_x/\rho V_w^2 X)$

Table I

Summary of Numerical Results, Uniform Injection Case

f"(0)	C	Re	F"(0)	F"(1)	$(C/C^*)^1$
.100	90000	$.13333 \times 10^{-3}$	6.0000	-6.000	1.0000
.200	5624.0	.0021345	6.0000	-5.999	1.0000
.300	1110.1	.01083	6.0050	-5.994	1.0021
.400	350.59	.034456	6.0157	-5.981	1.0066
.500	143.02	.085284	6.0389	-5.954	1.0165
.600	68.46	.18143	6.0829	-5.903	1.0351
.700	36.497	.35124	6.1602	-5.816	1.0683
.800	20.975	.64428	6.2934	-5.672	1.1261
.850	16.235	.86480	6.3932	-5.569	1.1700
.900	12.702	1.1618	6.5271	-5.438	1.2298
.950	10.023	1.5727	6.7111	-5.270	1.3136
1.000	7.9601	7.1656	6.9738	-5.051	1.4365
1.050	6.3491	3.0815	7.3724	-4.762	1.6304
1.100	5.0723	4.6732	8.0407	-4.375	--
1.120	4.6405	5.6978	8.4533	-4.184	--
1.140	4.2430	7.1594	9.0176	-3.970	--
1.160	3.8777	9.4212	9.8370	-3.732	--
1.180	3.5363	13.403	11.140	-3.472	--
1.190	3.3725	16.800	12.138	-3.334	--
1.200	3.2100	22.281	13.584	-3.190	--
1.205	3.1280	26.514	14.594	-3.114	--
1.210	3.0444	32.621	51.928	-3.036	0.9886
1.215	2.9577	42.196	17.800	-2.953	0.9898
1.216	2.9400	44.803	18.274	-2.936	0.9902
1.217	2.9217	47.743	18.792	-2.918	0.9904
1.218	2.9033	51.086	19.362	-2.900	0.9908
1.219	2.8846	54.920	19.995	-2.882	0.9910
1.220	2.8655	59.361	20.702	-2.863	0.9916
1.222	2.8260	70.754	22.404	-2.824	0.9925
1.224	2.7843	87.736	24.670	-2.783	0.9936
1.226	2.7393	114.21	27.900	-2.739	0.9948
1.228	2.6890	164.25	33.048	-2.689	0.9961
1.230	2.6293	291.28	43.345	-2.629	0.9976
1.231	2.5920	474.31	54.767	-2.592	0.9986
1.232	2.5415	1277.3	88.628	-2.542	0.9993
1.1322	2.5272	1933.1	108.59	-2.527	0.9995
1.2323	2.5188	2602.0	125.68	-2.519	0.9997
1.2324	2.5087	3980.8	155.00	-2.509	0.9998
1.232587	$\alpha^2/4$				

[1] C^* is the asymptotic value of C as Re→ 0 or Re→ ∞ given respectively by equations (14) and (40).

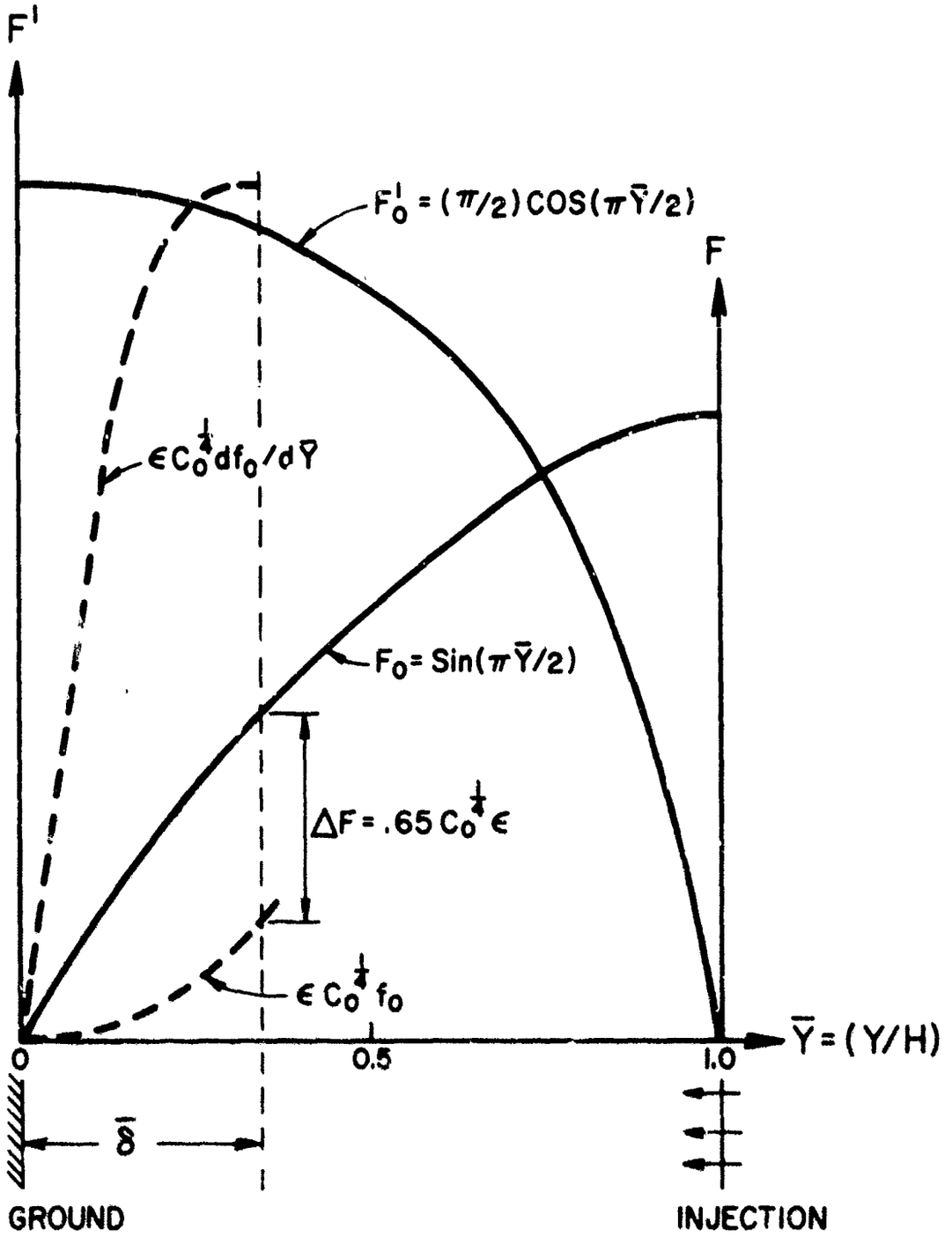

FIGURE 20. MATCHING OF THE INNER AND OUTER SOLUTIONS

With $f(0) = f'(0) = 0$, straightforward integration of the equation will bring f' to zero at, say, $\eta = \eta_o$ at which the value of f is, say, D. In view of the last two conditions of (18) it is obvious that

$$C^{1/4}\,Re^{1/2} = \eta_o$$
$$Re^{1/2}/C^{1/4} = D$$

and, of course,

$$C = (\eta_o/D)^2$$
$$Re = \eta_o D \qquad (19a,b)$$

The only inconvenience in the above scheme is that the Reynolds number is the output instead of being an input and may, therefore, be a little awkward. It goes without saying that $f''(0) = 1.2326$ corresponds to $Re = \infty$. The value of C is shown later to approach $\pi^2/4$. In short, for each value of $f''(0)$ assumed there results the following: Reynolds number, the pressure gradient parameter C, the velocity profile F' and the transverse pressure profile as supplied by equation (9). The results of these calculations are shown in Table 1 where the values of $F''(0)$ and $F''(1)$ are proportional to the shear stresses on the lower wall and the upper wall where the injection takes place. The reduction of the shear on the injection side is, of course, expected. Of interest are, however, the asymptotic value of the pressure parameter C and the shear on the injection side. Of equal significance is the fact that at Reynolds

numbers larger than 20 there is a rough relationship expressed by

$$F''(0) \sim Re^{1/2}$$

This relationship and the gradually steep velocity gradient for increasing Reynolds number on the solid wall as shown in Figures 15 to 19 suggest the existence of a thin boundary layer near the solid wall, i.e. the ground.

The pressure gradient parameter C defined in equation (9a) is plotted in Figure 20. It is clear that at the lower end of the Reynolds number scale the asymptotic formula $C = 12/Re$ holds whereas at the high end the C-value tends to be a constant which is shown in the next section to be $\pi^2/4$. The utilization of the C-values lies in their relation to the pressure distribution along the flow channel to be discussed later.

Asymptotically Large Reynolds Numbers Case

In common with the concept of the boundary layer theory the term F'''/Re in equation (10) is dropped and the resulting equation will be treated as the first-order external (to the boundary layer) solution. The resulting equation

$$F'^2 - FF'' = C \qquad (20)$$

has two solutions, i.e.

$$F = \pm\sqrt{C}\,y$$

and

$$F = A \cos y\sqrt{C/(A^2 + L^2)} + B \sin y\sqrt{C/(A^2 + B^2)}$$

The frist solution is, of course, a member of the second by letting A = 0 and B → ∞. This choice of A and B leading to a flat profile for F' is not consistent with the results of the numerical solution and is hence rejected. Now in the second solution there are three arbitrary constants which are to be determined by satisfying only three conditions* of (11). Since on the surface $\bar{y} = 0$ there is a boundary layer which is to be the solution of a boundary layer equation the conditions F'(0) = 0 is, therefore, dropped, the resulting solution is

$$F = \sin \bar{y}\sqrt{C} \tag{21}$$

where $\sqrt{C} = \pi/2$. The value of C appears to approach $(\pi^2/4)$ in Table I. This solution (external) gives F'(0) = $\pi/2$ and is, therefore, not valid near $\bar{y} = 0$. In order to construct a sequence of solutions in an orderly manner equation (10) is solved by the following expansion in the external region:

$$C^{1/4} = C_o^{1/4}\left[1 + C_1 \epsilon + C_2 \epsilon^2 + \ldots\right] \tag{22}$$

$$C_o = \pi^2/4 \text{ and } \epsilon = 1/\sqrt{Re} \tag{23}$$

$$F = F_o(\bar{y}) + \epsilon F_1(\bar{y}) + \epsilon^2 F_2(\bar{y}) \tag{24}$$

*The problem treated by White et al [4] is the one in which all their four conditions can be satisfied by three arbitrary constants.

After the usual procedure there results:

$$F_o'^2 - F_o F_o'' = C_o \tag{25}$$

$$2F_o' F_1' - F_o F_1'' - F_o'' F_1 = 4C_1 C_o \tag{26}$$

$$F_1'^2 + 2F_o' F_2' - F_2 F_o'' - F_1 F_1'' - F_2 F_o'' = C_o(4C_2+6C_1^2) + F_o'''' \tag{27}$$

In the boundary layer region, i.e. in the vicinity of $\bar{y} = 0$ the boundary layer coordinate $\eta_o = C_o^{1/4} \bar{y}/\varepsilon$ is used and expand the function F as

$$F = \varepsilon C^{1/4} \left[f_o(\eta_o) + \varepsilon f_1(\eta_o) + \varepsilon^2 f_2(\eta_o) + \ldots\right]$$
$$= \varepsilon C_o^{1/4} \left[f_o + \varepsilon(C_1 f_o + f_1) + \varepsilon^2 (f_2 + C_1 f_1 + C_2 f_o) + \ldots\right] \tag{28}$$

$$F'(\bar{y}) = C_o^{1/2} \left[f_o' + \varepsilon(C_1 f_o' + f_1') + \ldots\right] \tag{28a}$$

The composite function f_o, f_1, ... are determined by:

$$f_o'''' = f_o'^2 - f_o f_o'' - 1 \tag{29}$$

$$f_1'''' + f_o f_1'' - 2f_o' f_1' + f_o'' f_1 = -4C_1 - 2C_1 f_o f_o'' + 2C_1 f_o'^2 - C_1 f_o'''' \tag{30}$$

It is to be noted that equation (29) although the same form as equation (17) is in reality different in that the former is the boundary-layer equation subjected to the standard two-point boundary-value problem whereas the latter is valid for the entire channel and constitutes an eigen-value problem. Beginning with (25) one has

$$F_o = \sin \sqrt{C_o}\, \bar{y} \tag{31}$$

where the parameter C_o is taken to be $\pi/2$ in order to satisfy the condition $F(1) = 1$, hence

$$C_o = \pi^2/4 \tag{32}$$

Near the solid wall $\bar{y} = 0$ equation (31) gives a finite velocity $F_o'(0) = (\pi/2)$. This is to be remedied by allowing a boundary layer to exist near $\bar{y} = 0$ of the thickness $\bar{\delta}$ in which the velocity F' is to vary from 0 to $(\pi/2)$ at the edge of the boundary layer $\bar{\delta}$. This behavior is to be provided by the first term f_o in the expansion near $\bar{y} = 0$ as shown in equation (28). The governing equation (29) for f_o is, therefore, subjected to the boundary conditions

$$f_o(0) = 0;\ f_o'(0) = 0;\ \text{and}\ f_o'(C_o^{1/4}\bar{\delta}/\varepsilon) = 1$$

At asymptotically large Reynolds number, i.e. $\varepsilon \to 0$, the last condition is replaced by $f_o''(\infty) = 1$. The solution to equation (29) with these boundary conditions is, of course, the Falkner-Skan function with $f''(0) = 1.2326$ and the value of f_o at large arguments is asymptotically given by

$$f_o = \eta_o - 0.65$$

This composite nature of the function F comprised of equation (31) in the main bulk of the channel and the Falkner-Skan velocity distribution near the solid wall is illustrated in Figure 21. In the boundary layer region $\bar{y} = \bar{\delta}$ the dashed curve $\varepsilon\, C_o^{1/4} d\, f_o/d\bar{y} = C_o^{1/2}\, f_o'$ replaces F_o'.

The function F itself in this region is replaced by $\varepsilon\, C_o^{1/4}\, f_o$. However, this replacement i.e. $\varepsilon\, C_o^{1/4}\, f_o$ does not match the external stream function at the "junction" $\bar{y} = \bar{\delta}$. The disparity is given by

$$\Delta F = F_o\,(\bar{\delta}) - \varepsilon\, C_o^{1/4}\, f_o\,(C_o^{1/4}\,\bar{\delta}/\varepsilon)$$

Under the condition of $\bar{\delta} \to 0$ and $\bar{\delta}/\varepsilon \to \infty$ the disparity is obtained as

$$\Delta F = \sqrt{C_o}\,\bar{\delta} - \varepsilon\, C_o^{1/4}\left[C_o^{1/4}\,\delta/\varepsilon - 0.65\right] = 0.65\,\varepsilon\, C_o^{1/4}$$

Physically this quantity represents the transverse displacement velocity due to the boundary layer near the solid wall.

The mismatch of the stream function F at $\bar{y} = \bar{\delta}$ is now to be corrected in the outer region of εF_1, the second term of equation (24), such that the value of $F_o + \varepsilon F_1$ is equal to that of $\varepsilon\, C_o^{1/4}\, f_o$ at $\bar{y} = \bar{\delta}$. This is tantamount to the depression of the F-value, to be accomplished by εF_1, by an amount equal to ΔF. Consequently, the conditions of F_1 are:

$$F_1(1) = 0;\ F_1'(1) = 0;\ \text{and}\ F_1(\bar{\delta}) = -0.65\, C_o^{1/4}$$

For small $\bar{\delta}$ the last condition is replaced by

$$F_1(0) = -0.65\, C_o^{1/4} \tag{33}$$

The solution of equation (26) with the first two boundary conditions is

$$F_1(\bar{y}) = -2C_1 \left[(1-\bar{y})\sqrt{C_o} \cos \bar{y}\sqrt{C_o}\right] \tag{34}$$

and for (33) to hold one has:

$$C_1 = 0.65/(2C_o^{1/4}) \tag{35}$$

Now the process repeats itself i.e. $F_1(\bar{y})$ gives a slip velocity at $\bar{y} = 0$ as

$$\varepsilon F_1'(0) = 0.65\ C_o^{1/4}\ \varepsilon \tag{36}$$

which to be connected by the second term in the inner expansion of equation (28), i.e.,

$$\varepsilon\ C_o^{1/2} \left[C_1 f_o' + f_1'\right] = 0.65\ C_o^{1/4}\ \varepsilon$$

at $\eta_o \to \infty$. Hence, the boundary condition of f_1 at $\eta \to \infty$ is simply $f_1'(\ ) = C_1$. The other two conditions are, of course, $f_1'(0) = 0$ and $f_1(0) = 0$ and the solution f_1 satisfying equation (30) turns out to be

$$f_1 = C_1\ \eta_o\ f_o' \tag{37}$$

The outer stream function and the inner stream function at $\bar{y}$ = differ by

$$\Delta F = \left\{f_o(\bar{\delta}) + \varepsilon\ F_1(\delta)\right\} - \varepsilon C_o^{1/4} \left\{f_o(\infty) + \varepsilon \left[C_1 f_o(\infty) + f_1(\infty)\right]\right\}$$
$$= 0.65^2\ \varepsilon^2/2$$

which is used to determine the boundary condition for F_2 at $\bar{y} = \bar{\delta}$, i.e.

$$F_2(0) = -0.65^2/2$$

The function F_2 from equation (27) is found to be

$$F_2(\bar{y}) = -(C_1 \pi^2/2) \left[(1-\bar{y}) \sin(\bar{y}/2)\right] + (\pi/2) \left[4C_1 - 2C_2 - 3C_1^2\right] (1-\bar{y})\cos(\pi\bar{y}/2) - (\pi/2)\cos(\bar{y}/2)\int_{(\pi/2)}^{(\pi\bar{y}/2)} \left[\cos z(\sin z - z \cos z)/\sin^3 z\right] dz + (\pi/4) \left[\sin(\pi\bar{y}/2)-(\pi\bar{y}/2)\cos(\pi/2)\right] \left[(\cot(\pi y/2)/\sin(\pi\bar{y}/2))+\log \tan(\pi\bar{y}/4)\right] \quad (38)$$

The condition of $F_2(0) = -0.65^2/2$ is used to determine the coefficient C_2 as

$$2C_2 = 2C_1 - 3C_1^2 + (0.65^2/\pi) + \int_0^{\pi/2} \left[\cos z (\sin z - z \cos z) /\sin^3 z\right] dz$$

or

$$C_2 = 0.4337 \quad (39)$$

Up to the second order of ε, the pressure-gradient constant C may be expressed as

$$C = (\pi^2/4)(1 + 1.0373 \ \varepsilon + 2.1682 \ \varepsilon^2 \ldots) \quad (40)$$

and the shear stresses at $\bar{y} = 0$ and $\bar{y} = 1$ are given by the following asymptotic formulas

$$F''(0) = (C_o^{3/4}/\varepsilon) \left[1 + 2C_1 \varepsilon + \ldots\right] \quad (41)$$

$$F''(1) = (\pi^2/4) \left[1 - 4C_1 \varepsilon + 0(\varepsilon^3) + \ldots\right] \quad (42)$$

The pressure differential across the channel is given directly as

$$(p_{\bar{y}=1} - p_{\bar{y}=0}) = - \rho v_w^2/2 \tag{43}$$

The pressure gradient C, the shear stresses F"(0) and F"(1) and other pertinent quantities are shown in Table 1.

Figure (20) shows the variation of C vs. the injection Reynolds number. From an engineering calculation viewpoint the pressure distribution is given by

$$p = C \left[\rho v_w^2/2\right] (L^2 - x^2)/H^2 + p_a \tag{44}$$

where p_a is the ambient pressure and the use of this relation implies that the pressure difference <u>across</u> the channel width as given by equation (43) is negligible. At x = 0, the peak pressure is given by equation (44) with

$$p_c - p_a = C \left[\rho v_w^2/2\right] (L^2/H^2) \tag{45}$$

where p_c now denotes the cushion pressure. It is not possible or meaningful in the present case to construct the pressure parameter

$$(p_c - p_a)/(p_t - p_a)$$

where p_t is the total pressure in the trunk. The reason is that the injection rate, i.e., the rate of air flow through the trunk distribution-holes is a constant is only true at the choked condition. However, if one tentatively places the total (trunk) pressure as

$$p_t = p_c + 1/2\ \rho\ v_w^2$$

then the pressure coefficient

$$(p_c-p_a)/(p_t-p_a) = C(L^2/H^2)/\left[1 + C(L^2/H^2)\right] \ldots \qquad (46)$$

which is seen to be dependent on the Reynolds number. Under the almost contact condition between the ground and the trunk $L^2/H^2 \to \infty$, and the pressure coefficient becomes one.

IV. VARIABLE-INJECTION FLOW CASE

The analysis presented in Section III is valid when the rate of the bleed air-flow through the distribution holes along the cushion seal is uniform. In practice this is only true when the trunk pressure is at a very high pressure in the order of 50 to 100 psig so that the flow through the orifices is at a choked condition. Since this extreme condition is rarely encountered, it is, therefore, desirable to have a method available to account for the variable flow case so that more realistic cushion pressure can be estimated.

From a practical consideration the distribution of the bleed flow from the pneumatic trunk is affected by (1) the flow resistance across the "orifices," i.e. the orifice coefficient and (2) the pressure distribution in the flow channel. Thus the distribution of the bleed flow

along the channel cannot be determined until the pressure variation in the channel is known; the latter is in turn dependent upon the flow distribution or accumulation from the bleed-side of the wall. While it is possible to analyze the interaction as discussed above from a more exact fluid dynamic viewpoint it is more expedient to employ the concept of local similarity in treating the present problem.

The local similarity rule as applied to the channel flow problem is interpreted as follows: referring to Figure 2 the local pressure gradient p_x is determined by a local pressure gradient coefficient C which is in turn determined by the local Reynolds number ($v_w H/\nu$). The velocity distribution (u/u_a) is also determined by the local value of the Reynolds number. Mathematically this is expressed by

$$u = F'(\bar{y}) \int_o^x (v_w/H)dx \tag{47}$$

$$v = -v_w F(\bar{y}) \tag{48}$$

Equations (47) and (48) reduce to equations (6) and (7) when v_w is a constant.

Substitution of equations (47) and (48) into equation (1) there results

$$F'^2 - FF'' = -\left[H^2 p_x/\rho v_w dx\right] + (\nu/Hv_w)F''' \tag{49}$$

The first term on the LHS is now a function of x. This is because the Reynolds number ($v_w H/\nu$) is x-dependent in (49) but not so in equation (8) for the uniform injection case. In the present case the present gradient term in the brackets of equation (49) is only dependent on (Hv_w/ν). The fact that this is a practically acceptable procedure is justified on the basis that the average value of the convective terms on the LHS of equation (49) is nearly a constant. The pressure gradient p_x is dependent upon the friction resistance on the wall denoted by F"' in equation (49) and upon the momentum increase. The momentum increase is partly dependent upon the accumulated flow and partly upon the shape of the velocity distribution in the channel. Consequently, the integrated value from $\bar{y} = 0$ to $\bar{y} = 1$ of the convective terms of the LHS represents the influence of the shape factor or

$$\int_0^1 (F'^2 - FF'')\, d\bar{y} = 2 \int_0^1 F'^2 d\bar{y}$$

From Re = 0 to Re = ∞ this shape factor changes from 1.20 to ($\pi^2/8$). Since this change is minor and this variation is included in the local similarity rule the procedure is, therefore, valid.

Computation Procedure

With the pressure gradient parameter C defined in Table I for various local Reynolds number, the pressure gradient can be written as

$$\frac{dp}{dx} = -\left[\frac{\rho v_w \int_o^x v_w \, dx}{H^2}\right] C \qquad (50)$$

For flow with appreciable variations in density, it should be inside the integral.

It is assumed that the following data are known in advance:

L = length of channel, ft

H = ground clearance, ft

ν = air kinematic visco ity, ft^2/sec

p_t = trunk pressure, psfa

p_a = ambient pressure, psfa (2116.8 psfa or 14.7 psia)

Additionally, appropriate coefficients of discharge for flow through the distribution holes must be known. The procedure is essentially a cut-and-trial method. It begins with an assumed value of the pressure at x = o which is below the trunk pressure and above the ambient pressure.

For illustration let the bleed flow be determined from the simple orifice formula:

$$v_w = \left[C_d \, A_r \sqrt{2g_o(p_t - p)/\rho}\right] \qquad (51)$$

where A_r is the ratio of the orifice area to the seal area. For example if the orifices are placed 3 inches apart (center-to-center) on a square-pitch basis and the orifice

diameter is 2 inches, then $A_r = \left[2^2/4 \right] /3^2 = \pi/9$. Equation (51) gives the value of v_w at x = 0 which defines the Reynolds number ($v_w H/\nu$) at x = 0. From Table I the pressure gradient parameter C is obtained. Since the pressure gradient itself is zero at x = 0, the pressure at x = Δ may be calculated as

$$p_{(x=\Delta)} = p_{(x=0)} - (\rho v_w^2 C/H^2)\, \Delta^2/2 \qquad (52)$$

The next step is now to compute v_w at x = Δ by means of equation (51) and to compute the pressure gradient from equation (50) after Table I is used to obtain C. In this way the pressure at progressively large x can be numerically evaluated until at x = L the claculated pressure must match the ambient pressure. If the calculated pressure is higher than the ambient pressure then the assumed pressure at x = 0 is too large and a lower value must be tried.

A large number of computer runs were performed. The general ranges of the parameters were as follows: trunk pressure varied from 0.5 to 6.0 psig at 1.0 psi interval; the $C_d A_r$ (coefficient of discharge times the area ratio) varied from 0.003 to 0.27 at 0.003 interval; the ground clearance height H varied from 0.04 to 0.16 ft at 0.04 ft interval and the clearance-length ratio (H/L) varied from 0.05 to 1.0 at 0.05 interval.

Figures 21-a,b,c, contain the typical pressure variation along the channel-seal for an (H/L) ratio of 0.05, 0.10, and 0.15 respectively. The abscissa is the dimensionless distance (x/L) from the cushion-space and L is the length of the channel-seal. The ordinate shows the non-dimensional local pressure ratio $(P-P_c)/(P_t-P_a)$. The parameters are the values of the C_dA_r. For large values of C_dA_r the pressure distribution is within the flow channel almost constant indicating the phenomenon that air injection takes place only near the exit (ambient) side. It is significant to call attention to the fact that these non-dimensional pressure distribution is virtually independent of the trunk pressure at least from 0.5 to 6.0 psig and the ground clearance H from 0.04 to 0.15 ft. Over these ranges of the above-cited parameters the curves are identical and indistinguishable from one another. Numerical differences however do exist but only in the third significant digit.

Each curve in Figures 21-a,b,c, was used to obtain the average pressure within the channel seal. This averaged pressure when multiplied by the area of the seal gives additional lift to the vehicle which may be of an appreciable magnitude. The parameter shown on the ordinate of Figure 22-a,b, is $(\bar{P}_{av}-P_a)/(P_c-P_a)$ with the cushion gage pressure as the reference; P_{av} is the average channel pressure.

It is to be noted that Figures 22-a, and b are for two different trunk pressures of 6.0 and 2.0 psig and these two figures virtually duplicates each other.

From the pressure distribution like those in Figure 21-a, the value at (X/L) = 0 is the cushion pressure ratio based on the assumption of no air moisture in the cushion-air space. This cushion pressure ratio then depends on (H/L) and the C_dA_r-value. For example at H/L = .05 and C_dA_r = .03, .045... the cushion pressure ratios are 0.549, 0.790,... The latter values are tabulated in Table II and plotted in Figures 23-a,b, for the trunk pressure of 6.0 psig and 2.0 psig. These two figures are almost identical indicating its insensitivity to the trunk pressure. The last two figures are particulary important in that the overall performance of the cushion-lift can be directly obtained. As an illustration, consider the example:

Trunk pressure = 4.0 psig

Cushion-space area = 200 sq. ft.

Channel-seal length = 1 ft.

Vehicle weight = 100,000 lb.

C_dA_r = .21

The last value can be estimated from the geometrical spacing of the bleed holes located in the cushion-bag. The coefficient of discharge is usually in the range of 0.6 corresponding to

the orifice discharge coefficient. A more accurate estimate will be reported in Part II of this report to be published shortly.

From the preceding information it is possible to calculate the necessary cushion pressure for take-off operation.

$$P_c = 100{,}000/(200 \times 144) = 3.47 \text{ psig}$$

The cushion pressure ratio is therefore (3.47/4.0) = 0.868. From Figure 23a or 23b, the curve with $C_d A_r = 0.21$ gives a value of (H/L) = 0.20. For L = 1 ft, the ground clearance height H = 0.20 ft or 2.4 inches. Of course the information in Figure 23 can be used to determine the proper $C_d A_r$ if H is to be specified. This specifies the proper spacings of the bleed holes and subsequently the rate of discharge of bleed air.

A general computer program is attached in Appendix. The computer program requires the following input values: $C_d A_r$; trunk pressure, ambient pressure, both in psia; seal length in ft.; ground clearance H in ft; and the kinematic viscosity of air (≈ 0.00015 ft^2/sec). These data are to be read by the computer program on a single punch data card (format 6F10.2) for each configuration. After one run is completed the program will read the next card which may contain different parametric inputs for the next run. The program continues in this manner until it reads a blank card which must be attached next to the last data card.

The output of the program for each run consists of two parts: the first part is a tabulation of the local pressure ratio $(P-P_a)/(P_t-P_a)$, the local injection velocity (Prorated over the entire seal area) in ft per sec, the local pressure gradient constant C, and the local Reynolds number at about 39 stations of increasing (x /L) values where x is the distance from the cushion-space. The second part gives the average pressure (gage) in the seal area in its ratio to the gage trunk pressure, the actual injection flow rate in cfs per ft of depth of the cushion space.

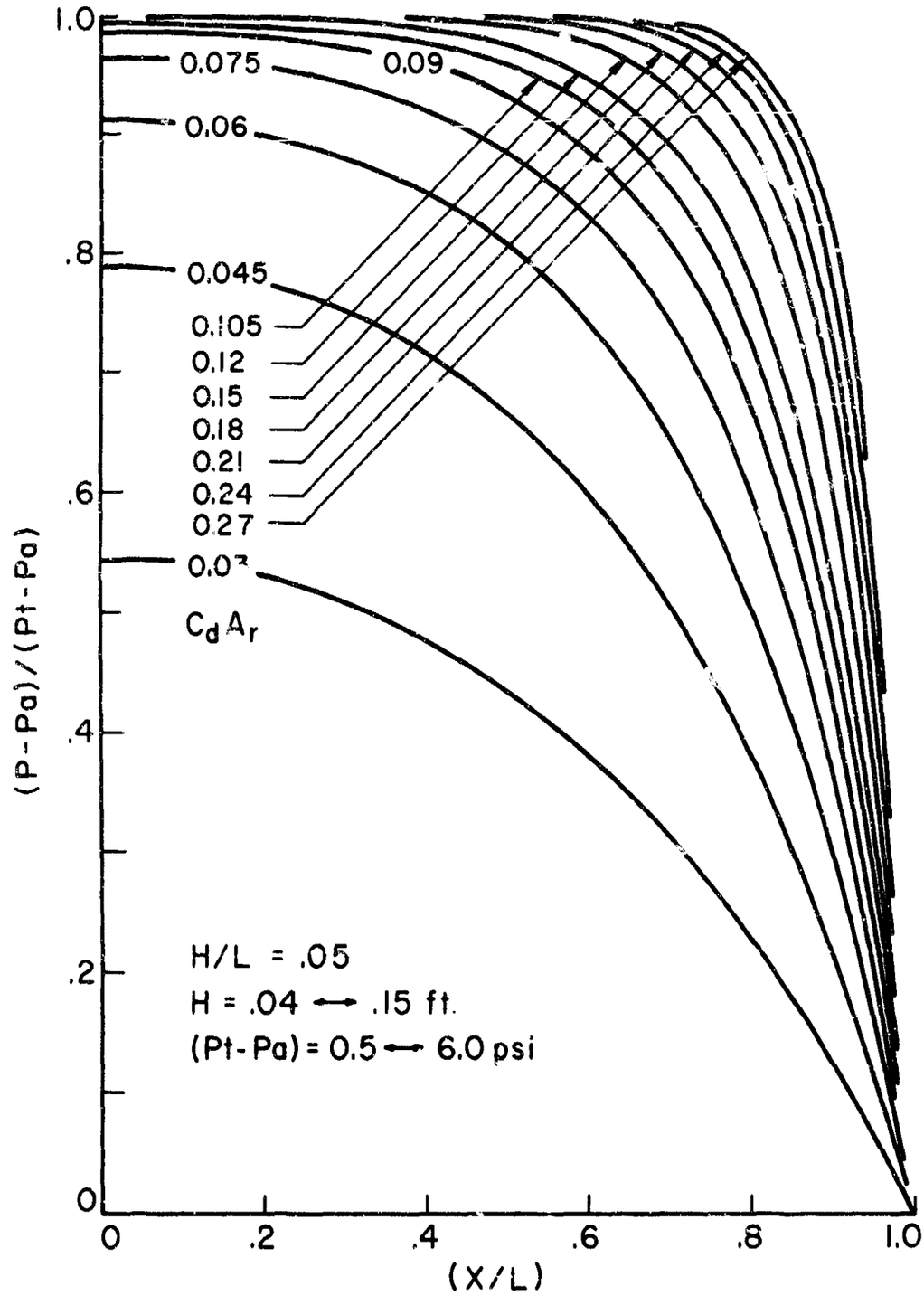

FIGURE 21a. Pressure Variation Along Channel-Seal

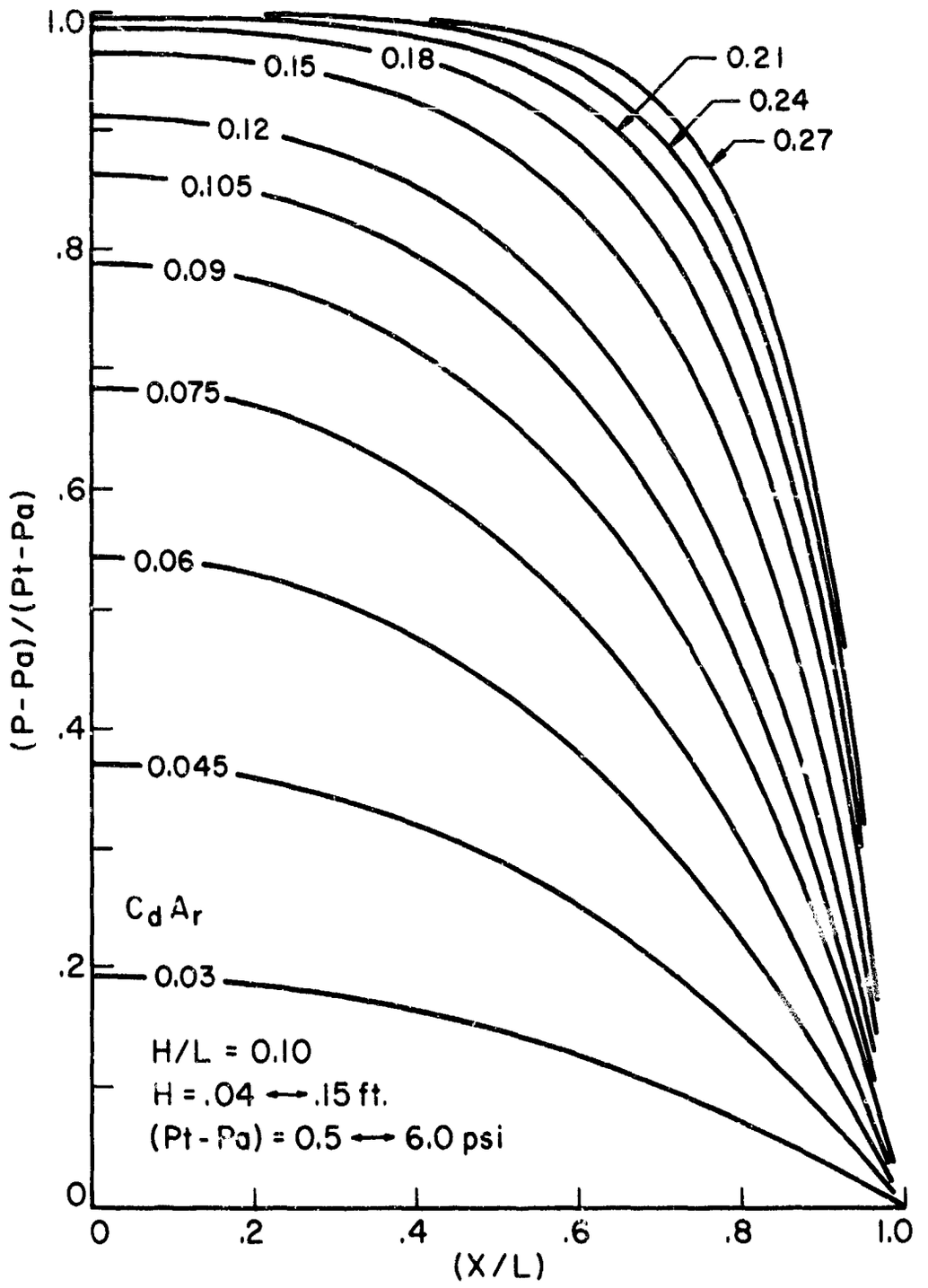

FIGURE 21 b. Pressure Variation Along Channel-Seal

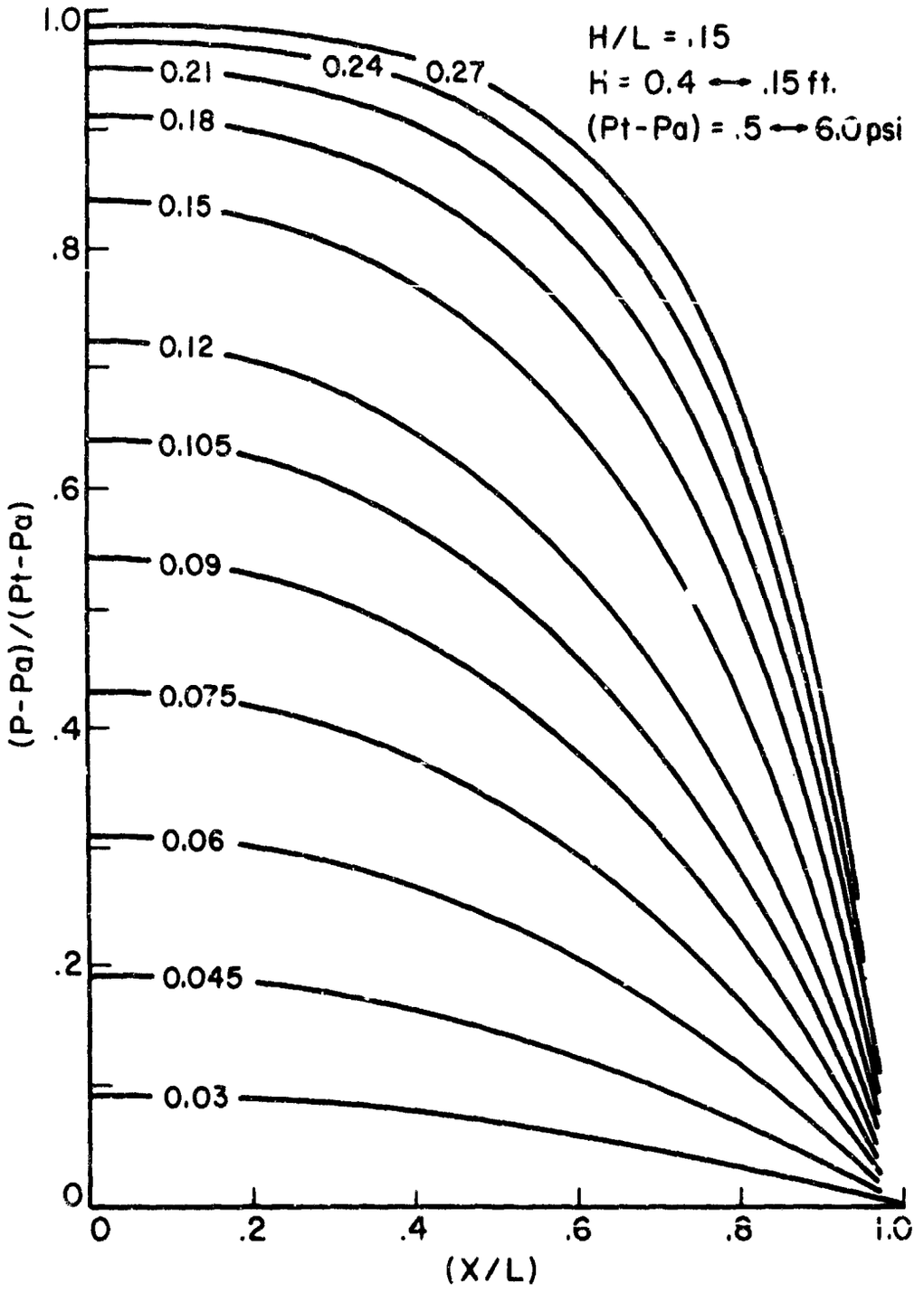

FIGURE 21c. Pressure Variation Along Channel-Seal

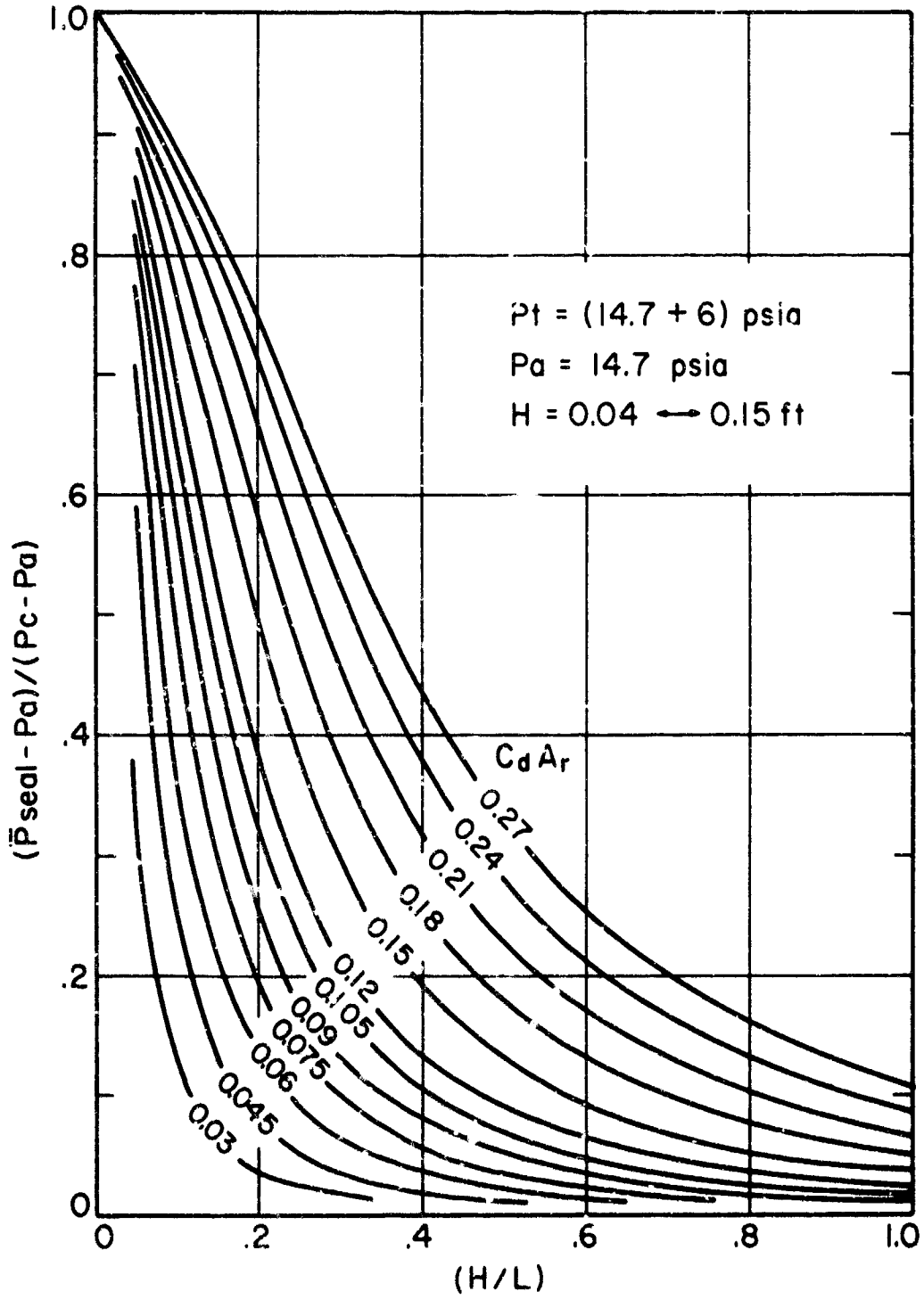

FIGURE 22 a. Average Seal Pressure As A Function Of Area Ratio And Ground-Clearance

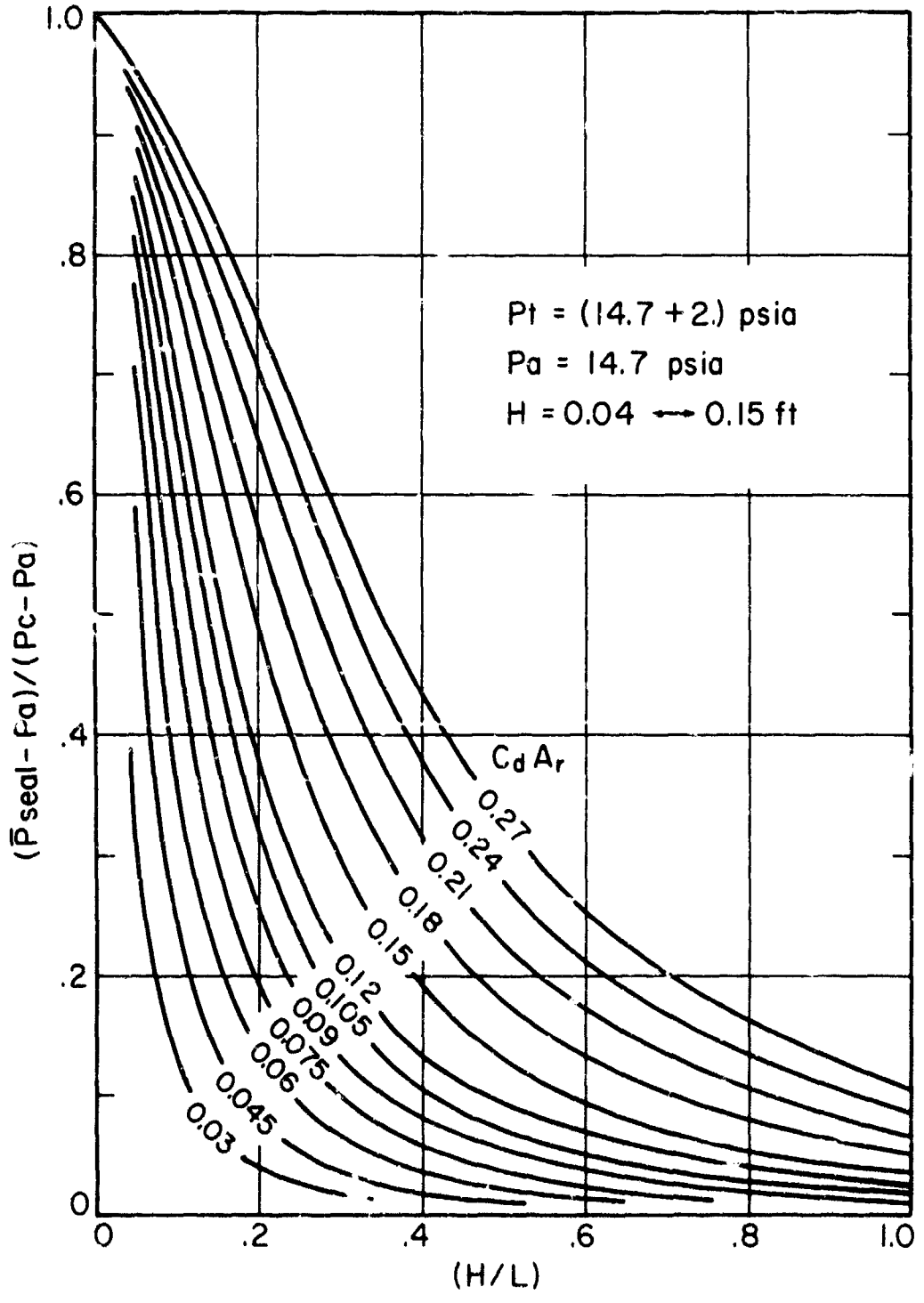

FIGURE 22 b. Average Seal Pressure As A Function Of Area Ratio And Ground-Clearance

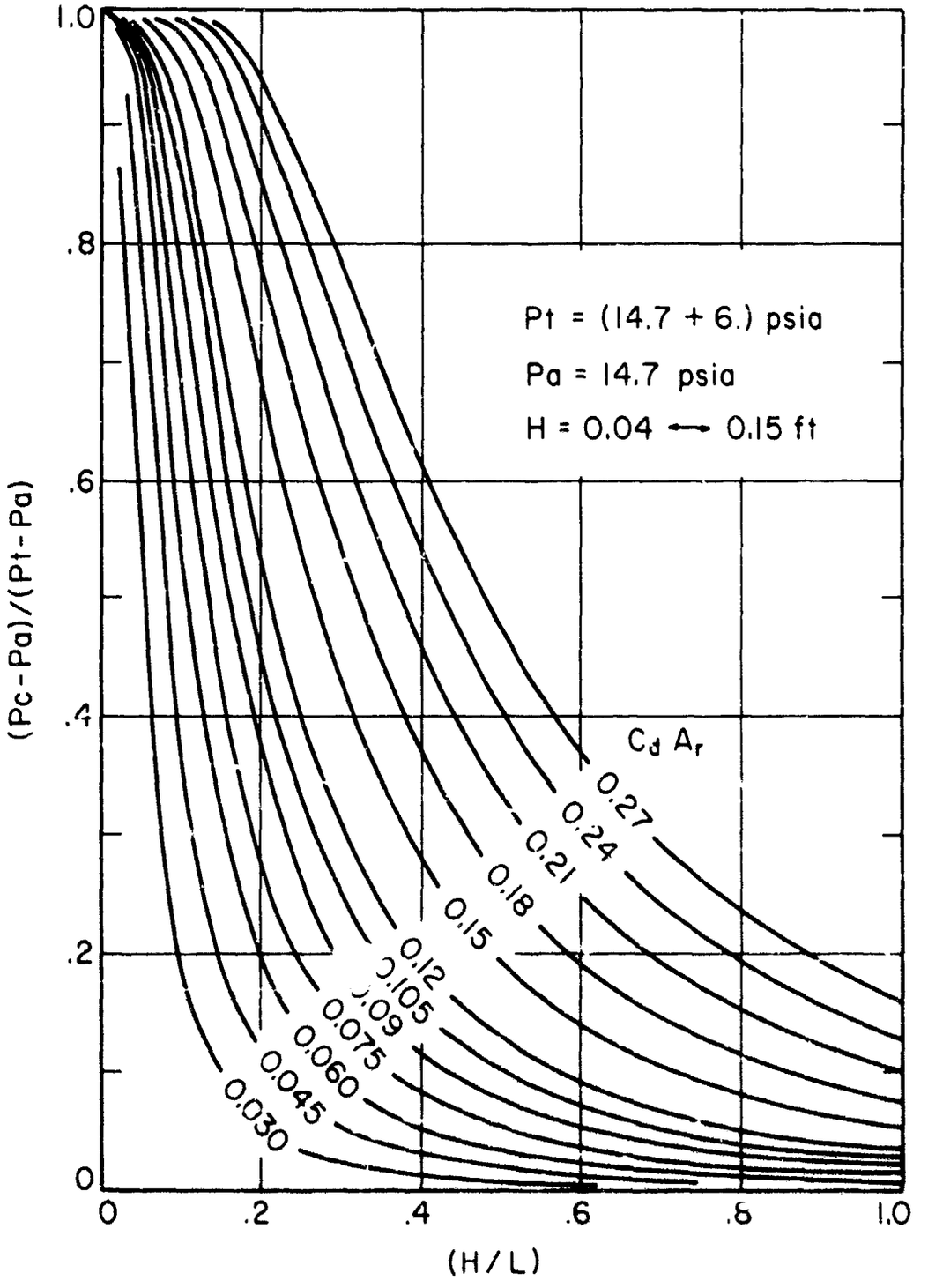

FIGURE 23a Cushion Pressure Ratios As A Function Of Area-Ratio And Ground-Clearance

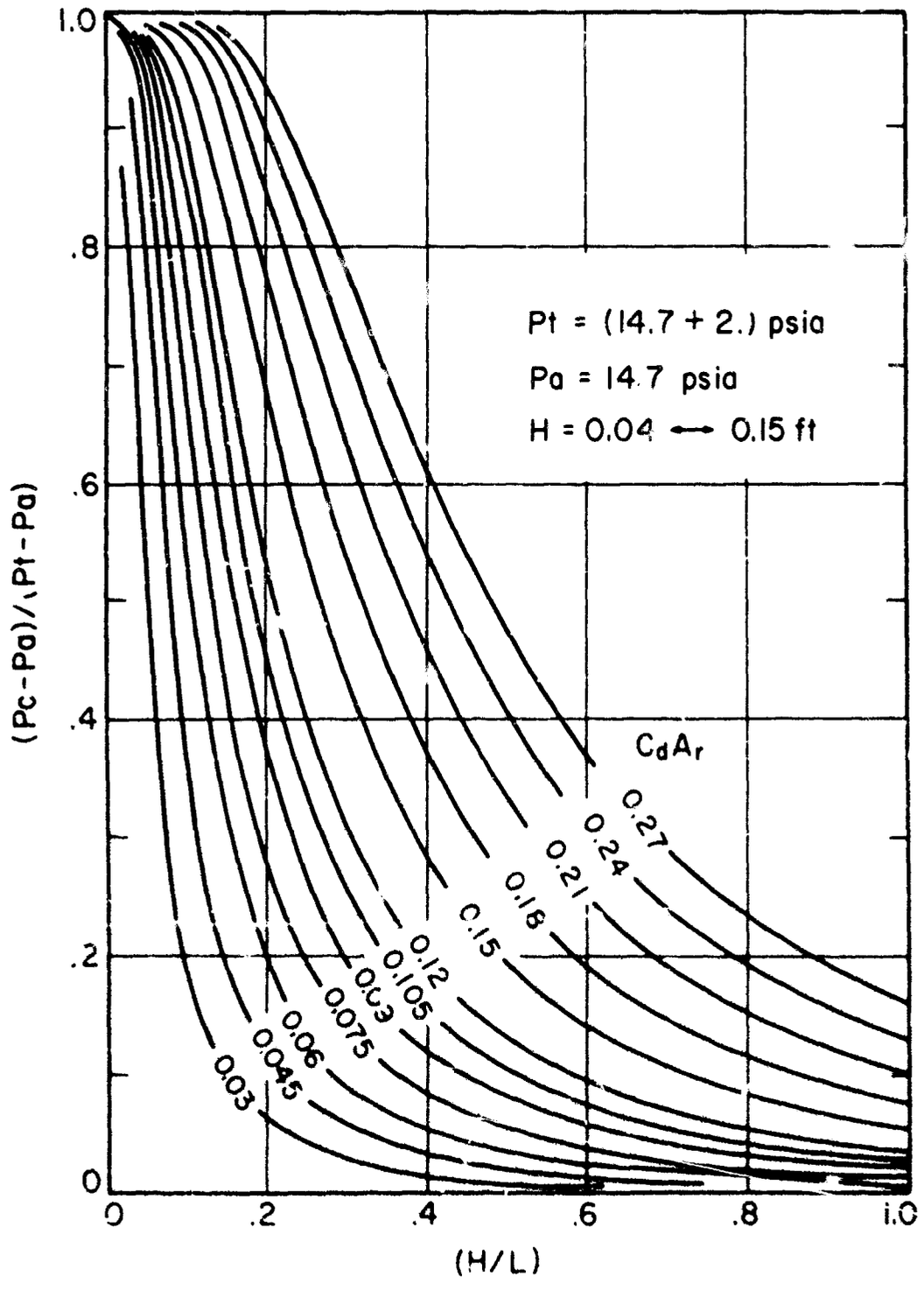

FIGURE 23 b. Cushion Pressure Ratios As A Function Of Area-Ratio And Ground-Clearance

TABLE II
COMPUTER CUSHION PRESSURE COEFFICIENTS
BASED ON VISCOUS THEORY

C_dA_r (H/L)	0.030	0.045	0.060	0.075	0.090	0.105
0	1.0	1.0	1.0	1.0	1.0	1.0
0.05	0.544	0.790	0.912	0.965	0.986	0.994
0.10	0.194	0.371	0.543	0.684	0.789	0.862
0.15	0.093	0.1 3	0.311	0.430	0.543	0.640
0.20	0.054	0.116	0.193	0.280	0.369	0.459
0.25	0.035	0.076	0.130	0.193	0.261	0.333
0.30	0.024	0.054	0.093	0.139	0.192	0.250
0.40	0.014	0.031	0.053	0.082	0.115	0.152
0.50	0.0088	0.0198	0.0347	0.0533	0.0759	0.101
0.60	0.0061	0.0137	0.0242	0.0375	0.0534	0.0716
0.70	0.0044	0.0101	0.0178	0.0277	0.0397	0.0533
0.80	0.0035	0.0078	0.0138	0.0213	0.0305	0.0413
0.90	0.0027	0.0061	0.0109	0.0169	0.0241	0.0328
1.00	0.0022	0.0049	0.0088	0.0136	0.0196	0.0267

TABLE II (cont.)

C_dA_r (H/L)	0.120	0.150	0.180	0.210	0.240	0.270
0	1.000	1.000	1.000	1.000	1.000	1.000
0.05	0.988	0.999	1.000	1.000	1.000	1.000
.10	0.912	0.964	0.986	0.994	0.998	0.999
0.15	0.723	0.841	0.911	0.952	0.974	0.986
0.20	0.542	0.683	0.788	0.862	0.911	0.943
0.25	0.406	0.542	0.657	0.751	0.821	0.873
0.30	0.310	0.430	0.541	0.640	0.722	0.788
0.40	0.192	0.279	0.368	0.458	0.541	0.616
0.50	0.129	0.193	0.262	0.333	0.406	0.475
0.60	0.0919	0.139	0.191	0.249	0.308	0.370
0.70	0.0689	0.105	0.146	0.192	0.242	0.292
0.80	0.0533	0.0817	0.115	0.151	0.192	0.235
0.90	0.0423	0.0653	0.0923	0.122	0.156	0.191
1.00	0.0345	0.0532	0.0756	0.101	0.129	0.160

REFERENCES

1. T. D. Earl, AIR-CUSHIONED LANDING GEAR FEASIBILITY STUDY, AF FDL-TR-67-32, May, 1967, BELL-Aerosystems Company.

2. S. W. Yuan and A. Finkelstein, Laminar Pipe Flow with Injection and Suction Through a Porous Wall, Proceedings of Heat Transfer and Fluid Mechanics Institute, 1955.

3. M. Morduchow, On Laminar Flow Through a Channel or Tube with Injection; Application of Method of Average. Quarterly of Applied Mathematics, 1956, p. 361.

4. F. M. White, Jr., et al. Laminar Flow in a Uniform Porous Channel, Journal of Applied Mechanics, 1959.

APPENDIX: FORTRAN COMPUTER PROGRAM

```
C******INSTRUCTION
C******COEFD IS PRODUCT OF ORIFICE COEF AND AREA RATIO
C******PTRNK IS THE TRUNK PRESSURE IN PSI ABSOLUTE
C******PAMB IS ATMOSPHERIC PRESSURE IN PSI ABSOLUTE
C******EL IS THE SEAL CHANNEL LENTH IN FEET
C******H IS THE SEAL HEIGHT IN FEET
C******VISC IS THE KINEMATIC VISCOSITY OF AIR IN FT SQ PER SEC
C****** KINEMATIC VIS OF AIR=15.E-05 APP AT 40 DEG F
C******ENTER THESE DATA ON ONE CARD FORMAT 6F10.2 FOLLOWED BY A BLANK CARD
      DIMENSION ROOT(26),REV(26)
      DIMENSION CP(100),XL(100),VB(100)
      DIMENSION CO(100),REY(100)
      PIE=3.141593
      ROOT( 1)=        0.120050E 02
      REV( 1)=        0.213452E-02
      ROOT( 2)=        0.120252E 02
      REV( 2)=        0.108318E-01
      ROOT( 3)=        0.120797E 02
      REV( 3)=        0.344548E-01
      ROOT( 4)=        0.121977E 02
      REV( 4)=        0.852799E-01
      ROOT( 5)=        0.124214E 02
      REV( 5)=        0.181423E 00
      ROOT( 6)=        0.128186E 02
      REV( 6)=        0.351221E 00
      ROOT( 7)=        0.135123E 02
      REV( 7)=        0.644229E 00
      ROOT( 8)=        0.147568E 02
      REV( 8)=        0.116179E 01
      ROOT( 9)=        0.172369E 02
      REV( 9)=        0.216546E 01
      ROOT(10)=        0.195640E 02
      REV(10)=        0.308130E 01
      ROOT(11)=        0.237158E 02
```

```
      REV(11)=          0.467266E 01
      ROOT(12)=          0.264409E 02
      REV(12)=          0.569706E 01
      ROOT(13)=          0.303729E 02
      REV(13)=          0.715814E 01
      ROOT(14)=          0.354713E 02
      REV(14)=          0.914947E 01
      ROOT(15)=          0.473848E 02
      REV(15)=          0.133990E 02
      ROOT(16)=          0.714995E 02
      REV(16)=          0.222727E 02
      ROOT(17)=          0.828966E 02
      REV(17)=          0.265008E 02
      ROOT(18)=          0.992410E 02
      REV(18)=          0.325965E 02
      ROOT(19)=          0.124662E 03
      REV(19)=          0.421437E 02
      ROOT(20)=          0.169836E 03
      REV(20)=          0.592635E 02
      ROOT(21)=          0.242902E 03
      REV(21)=          0.872305E 02
      ROOT(22)=          0.439941E 03
      REV(22)=          0.163586E 03
      ROOT(23)=          0.760271E 03
      REV(23)=          0.289170E 03
      ROOT(24)=          0.121436E 04
      REV(24)=          0.468290E 03
      ROOT(25)=          0.174460E 04
      REV(25)=          0.678375E 03
      ROOT(26)=          0.314547E 04
      REV(26)=          0.123617E 04
      NRD=5
      M=6
   16 FORMAT(8F10.2)
```

```
    1 CONTINUE
      READ(NRD,16) COEFD,PTRNK,PAMB,EL,H,VISC
  333 FORMAT(/3X,3HNO.,7X,5H(X/L),5X,14H(P-PA)/(PT-PA),6X,21HVB(FT/SEC)(
     *INJ VELOC),3X,16HPRESS-GRAD CONST,5X,12HLOCAL REY NO)
  111 FORMAT(I6,4X,F10.5,3X,F12.5,8X,L16.6,2E20.4)
      IF(COEFD) 1111,1111,2
 1111 CALL EXIT
    2 CONTINUE
      DXREF=EL/H/38.
      NCT=0
      HOL=H/EL
      WRITE(M,1125) COEFD,PTRNK,PAMB,EL,H,HOL
 1125 FORMAT(1H1///13H INPUT VALUES,18H:  (COEF.DISC)*AR=,F12.5, 5X, 18H
     *TRUNK PRESS(PSIA)=,F12.5, 5X,20HAMBIENT PRESS(PSIA)=,F12.5/8X,22HL
     *ENGTH OF CHANNEL(FT)=,F12.5,5X,22HHEIGHT(CLEARANCE)(FT)=,F10.5, 9H
     *   (H/L)=,F9.6)
      PTRNK=PTRNK*144.
      PAMB=PAMB*144.
C*****CONVERTING PTRNK PAMB FROM PSIA INTO PSFA
      RHO=.0765*(PTRNK+PAMB)*.5/(14.7*144.)
      VNOT=COEFD*SQRT(2.*32.17*(PTRNK-PAMB)/RHO)
      RE=VNOT*H/VISC
      MAX=0
      MIN=0
      DPMAX=PTRNK-PAMB
      DPHIG=DPMAX
      XSHFT=0.
      DPMIN=.1E-33
      DPLOW=0.
      DPTRY=DPMIN
  101 CONTINUE
      DO 1101 LM=1,100
      CO(LM)=0.
      REY(LM)=0.
```

```
      XL(LM)=0.
      CP(LM)=0.
 1101 VB(LM)=0.
      I=0
      DPUSE=DPTRY
      VSTAR=0.
      XOL=0.
  155 VW=COEFD*SQRT(2.*32.17*DPUSE/RHO)
      I=I+1
      VST=VSTAR*VNOT
      XPUSE=PTRNK-DPUSE
      REXV=RE*VW/VNOT
      IF(REXV-REV(1)) 21,21,23
   21 CX    =12.+(ROOT(1)-12.)*(REXV/REV(1))
      GO TO 24
   23 IF(REXV-REV(26)) 22,20,20
   20 TX=ROOT(26)*4./(PIE**2*REV(26))
      GM=(TX-1.)*SQRT(REV(26))
      CX    =REXV*(PIE**2/4.)*(1.+GM/SQRT(REXV))
      GO TO 24
   22 DO 122 J=1, 25
      PR=(REXV-REV(J))*(REXV-REV(J+1))
      IF(PR) 26,261,122
  261 IF(REXV-REV(J)) 361,461,361
  461 CX=ROOT(J)
      GO TO 24
  361 CX=ROOT(J+1)
      GO TO 24
  122 CONTINUE
   26 CX    =ROOT(J)+(ROOT(J+1)-ROOT(J))*(REXV-REV(J))/(REV(J+1)-REV(J))
   24 CONTINUE
      DPDX=(VSTAR/RE)*CX
    7 FORMAT(8H  XSHFT=,F10.4,3X,
     *54HVALUES OF (X/H) LESS THAN THAT,ALL VW=0., PRESS CONST./)
```

```
      IF(I-1) 127,227,127
  227 CONTINUE
      NCT=1
      CO(NCT)=CX/REXV
      REY(NCT)=REXV
      XL(NCT)=XOL/(EL/H)
      VB(NCT)=VW
      CP(NCT)=(XPUSE-PAMB)/(PTRNK-PAMB)
      DELTA=.001*(EL/H)
  337 DELTA=DELTA*.5
      XREF=DXREF
      XOLT=XOL+DELTA
      DP=(RHO*VW*VISC/(2.*32.17*H))*DELTA**2*CX
      DPUSX=DPUSE+DP
      IF(DP-.0001*DPMAX) 187,187,337
  187 VSTAR=VSTAR+(VW/VNOT)*DELTA
      XOL=XOLT
      DPUSE=DPUSX
      GO TO 155
  127 CONTINUE
      DELTA=.005*(EL/H)
 1171 IF(REXV-.1) 2271,2271,3371
 2271 DP=VSTAR*CX*(RHO*VNOT*VISC/(32.17*H))*DELTA
      GO TO 4471
 3371 DP=DPDX*DELTA*RHO*VNOT**2/32.17
 4471 CONTINUE
      IF(DP-.005*DPMAX) 1175,1175,1173
 1173 DELTA=DELTA*.5
      GO TO 1171
 1175 DPUSX=DPUSE+DP
      XOLT=XOL+DELTA
      IF(DPUSX-DPMAX) 12,345,345
   12 IF(XOLT-(EL/H)) 901,9023,9023
  901 CONTINUE
```

```
      XOL=XOLT
      DPUSE=DPUSX
      VSTAR=VSTAR+(VW/VNOT)*DELTA
      IF(XOLT-XREF) 71,71, 471
  471 NCT=NCT+1
      NMAX=NCT
      CO(NCT)=CX/REXV
      REY(NCT)=REXV
      XL(NCT)=XOL/(EL/H)
      VB(NCT)=VW
      CP(NCT)=(DPMAX-DPUSX)/(PTRNK-PAMB)
      XREF=XREF+DXREF
   71 CONTINUE
      GO TO 155
  345 IF(XOLT-(EL/H)) 905,9034,9034
 9034 IF(DPFIN-DPMAX) 9023,9023,904
 9023 MIN=MIN+1
      DPLOW=DPTRY
 9044 CONTINUE
      DXRAT=((EL/H)-XOL)/DELTA
      DPFIN=DPUSE+DP*DXRAT
      NCT=NCT+1
      NMAX=NCT
      CO(NCT)=CX/REXV
      REY(NCT)=REXV
      XL(NCT)=1.
      VB(NCT) VW
      CP(NCT)=(DPMAX-DPFIN)/DPMAX
      VSTAR=VSTAR+(VW/VNOT)*DELTA*DXRAT
      GO TO 415
  904 MAX=MAX+1
      IF(DPTRY-DPMIN) 1905,1905,1906
 1906 CONTINUE
      DPHIG=DPTRY
```

```
      GO TO 9044
  415 DPTRY=.5*(DPHIG+DPLOW)
      IF(MIN*MAX, 416,404,416
  416 ER=(DPHIG-DPLOW)/DPTRY
      IF(ER-.1E-4) 505,505,404
  404 GO TO 101
  505 CONTINUE
      VOL=H*VNOT*VSTAR
      WRITE(M,333)
      WRITE(M,111)(L,XL(L ,CP(L),VB(L),CO(L),REY(L),L=1,NMAX)
      IF(XSHFT) 177,177,1771
 1771 WRITE(M,7777)
  177 CONTINUE
 7777 FORMAT(88H   FOR (X/L) LESS THAN THE FIRST VALUE (P-PA)/(PT-PA) IS
     * UNITY AND VB IS CONSTANT=VB(1).)
      PAV=CP(1)*(XL(1))
      DO 1234 L=2,NMAX
 1234 PAV=PAV+(CP(L)+CP(L-1))*.5*(XL(L)-XL(L-1))
      RATIO=VOL/(VNOT*EL)
      WRITE(M,4444) PAV,RATIO,VOL
 4444 FORMAT(29H   ***OTHER TECHNICAL DATA***/6X,59H(AVERAGE GAGE PRESSU
     *RE OVER SEAL AREA/TRUNK GAGE PRESSURE)=F10.4/6X,52H(AVE INJ BLEED
     *VEL/MAX INJ BLEED VEL-AT OUTER EDGE-)=,F10.4/6X,43HACTUAL FLOW RAT
     *E(CU FT/SEC PER FOOT DEPTH)=,E20.4)
      WRITE(M,4567)
 4567 FORMAT( 46H   *** NOTE  P =LOCAL PRESSURE IN CHANNEL SEAL/13X,19HP
     *A=AMBIENT PRESSURE/13X,17HPT=TRUNK PRESSURE/13X,53HVB=BLEED INJ VE
     *L PRORATED OVER TOTAL SEAL AREA IN FPS/13X,53HX =DISTANCE FROM CUS
     *HION SPACE TOWARD AMBIENT IN FEET/13X,21HL =SEAL LENTH IN FEET)
      WRITE(M,222)
  222 FORMAT(18H ***END OF ONE RUN)
      GO TO 1
  905 IF(DPTRY-DPMIN) 1905,1905,1907
 1907 MAX=MAX+1
```

```
      DPHIG=DPTRY
      GO TO 415
 1905 DPRAX=(DPMAX-DPUSE)/DP
      DXRAX=DELTA*DPRAX
      VSTAR=VSTAR+(VW/VNOT)*DXRAX
      XSHFT=(EL/H)-(XOL+DXRAX)
      DO 789 J=1,NMAX
      I=NMAX+1-J
      CP(I+1)=CP(I)
      VB(I+1)=VB(I)
      REY(I+1)=REY(I)
      CO(I+1)=CO(I)
      XL(I+1)=XL(I)+XSHFT/(EL/H)
  789 CONTINUE
      XL(1)=0.
      NMAX=NMAX+2
      XL(NMAX)=1.
      CP(NMAX)=0.
      VB(NMAX)=VB(NMAX-1)
      REY(NMAX)=REY(NMAX-1)
      CO(NMAX)=CO(NMAX-1)
      WRITE(6,7) XSHFT
      GO TO 505
      END
```